International Workshop
Infinite and Finite Nuclear Matter
(INFINUM-2025)

May 12 - 16, Dubna, JINR

Status and perspectives of the MPD detector program

V. Riabov for the MPD Collaboration

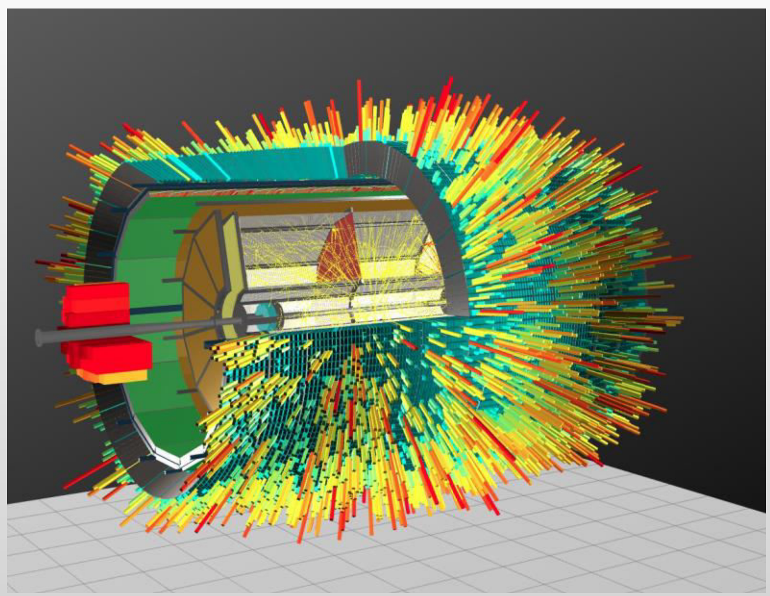

Heavy-ion collisions

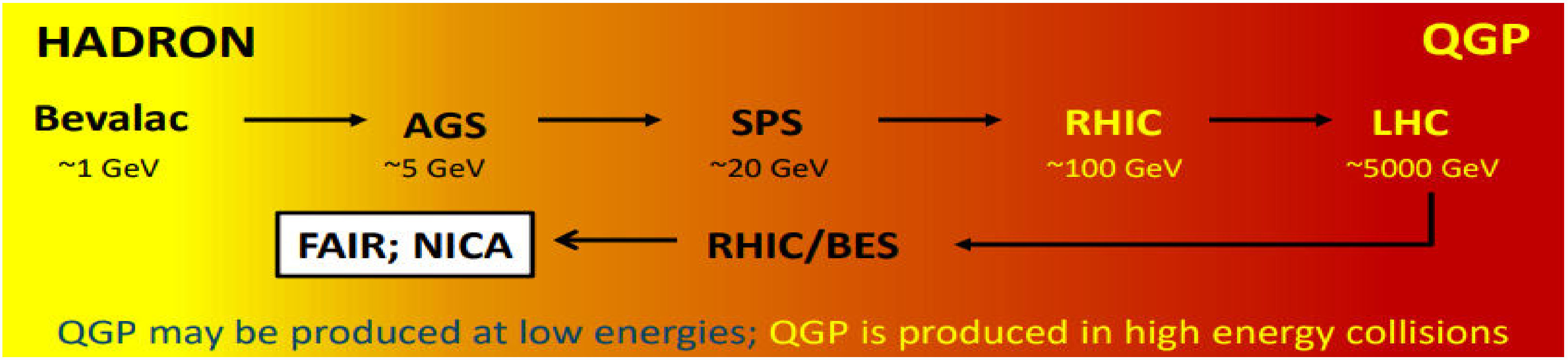

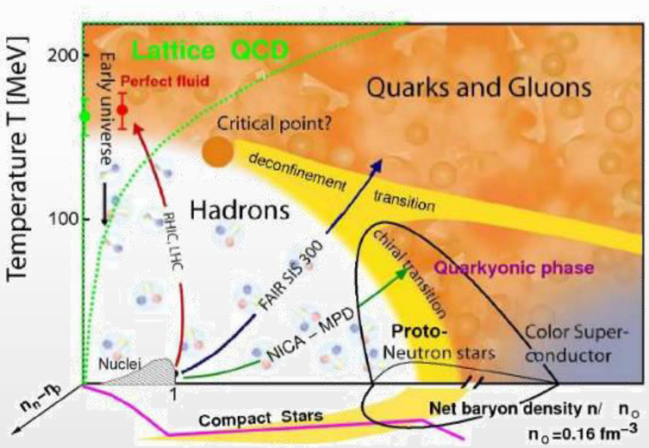

High beam energies ($\sqrt{s_{NN}}$ > 100 GeV)

High temperature:
Early Universe evolution

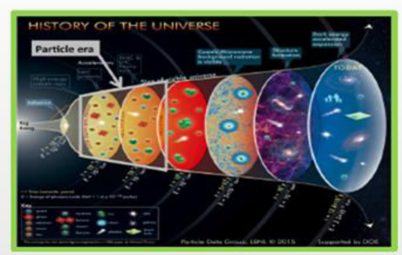

Low beam energies ($\sqrt{s_{NN}}$~ 10 GeV)

High baryon density:
Inner structure of
compact stars

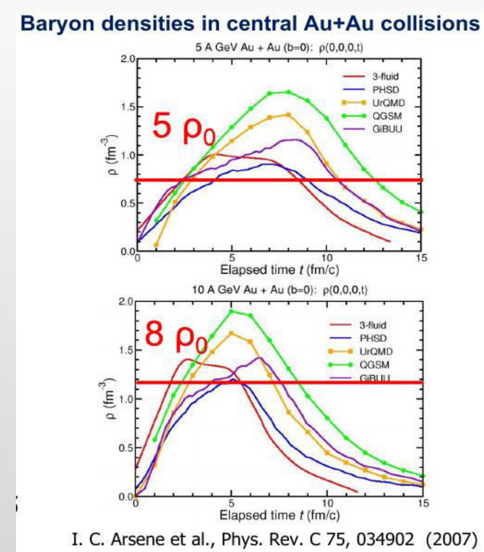

- At $\mu_B \sim 0$, smooth crossover (lattice QCD calculations + data)
- At large μ_B, 1st order phase transition is expected → QCD critical point
- MPD @NICA → study QCD medium at extreme net baryon densities

QCD critical point: predictions/estimations

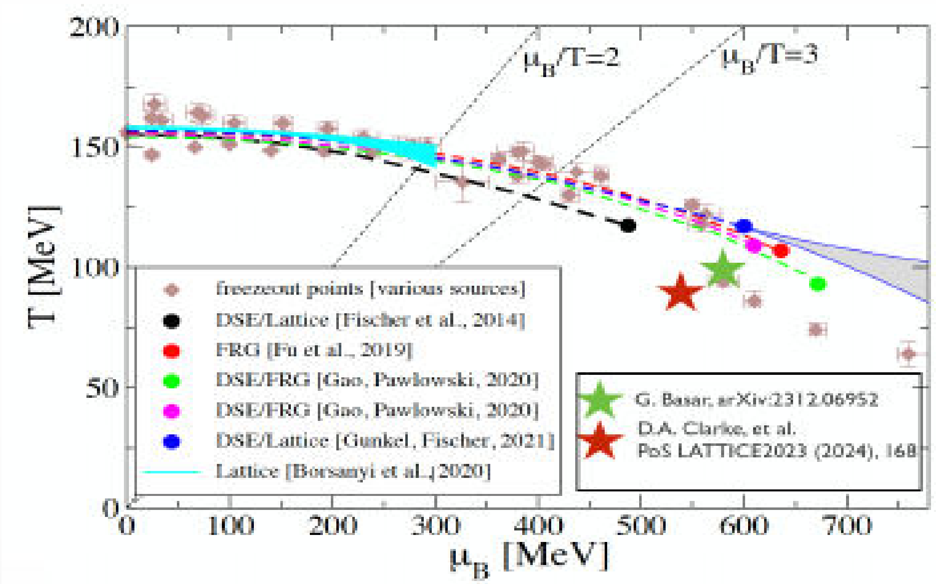

M. Hippert et al., Phys. Rev. D 110, 094006 (2024)

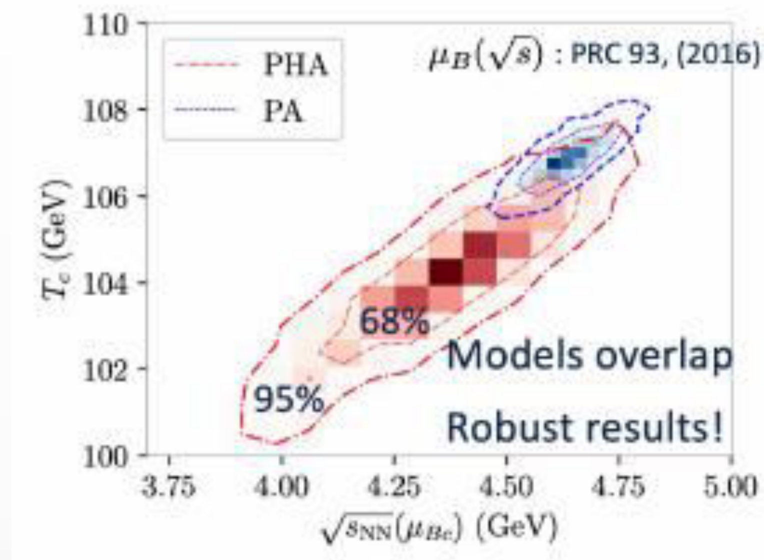

Method	μ_c (MeV)	T_c (MeV)
Holography + Bayesian	560 - 625	101 - 108
FRG/DSE	495 - 654	108 - 119
Lee-Yang edge singularities	500 - 600	100 - 105
Lattice QCD	$\mu_c/T_c > 3$	F. Karsch et al.
Summary	**495 - 654**	**100 - 119**

(μ_c, T_c) = (495 - 654, 100 - 119) MeV → $3.5 < \sqrt{s_{NN}} < 4.9$ GeV

BM@N: $\sqrt{s_{NN}}$= 2.3 - 3.3 GeV
MPD: $\sqrt{s_{NN}}$= 2.4 - 11 GeV

- BM@N and MPD in the collision energy range of the predicted CEP location.

Heavy-ion collisions and cosmology

- Nature of matter at extreme density (up to 5-10 ρ_0)

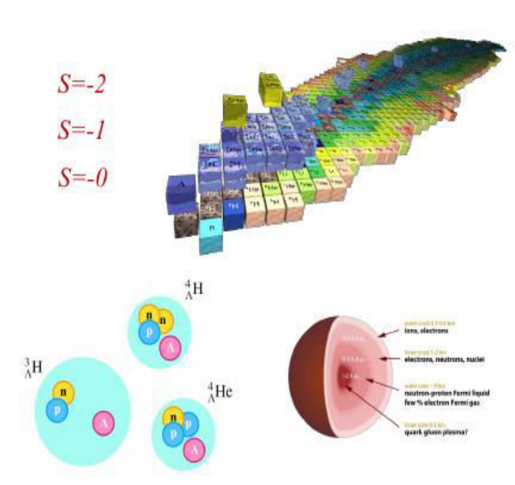

PRL**114**, 092301(2015), HYP2018, 1512.06832, 1711.07521

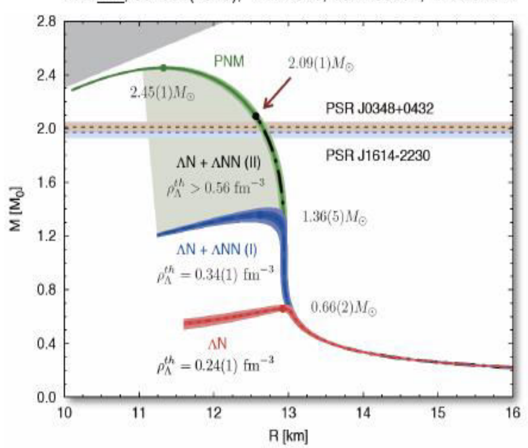

Hyperon and hyper-nuclei measurements in HIC → hyperon–nucleon interactions (NY, YNN) → key to understanding the EoS at high baryon density and inner structure of neutron star.

- Neutron star mergers

LIGO and Virgo Collaborations, Phys. Rev. Lett. 119 (2017) 16, 161101
Nature Phys. 15 (2019) 10, 1040-1045

Gravitational wave signal

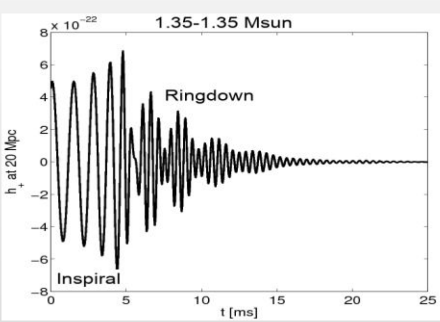

Neutron star mergers

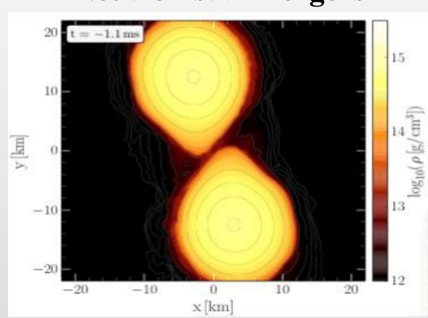

HIC: Au+Au 1.25 AGeV

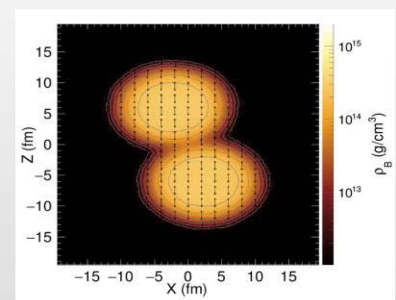

- ✓ Gravitational wave detection from GW170817, confirmation by astronomical observations
- ✓ T < 70 MeV, $\rho \sim 3\rho0$ → about the same conditions as achieved in HIC in the laboratory
- ✓ Source of heavy elements including Au, Pt, U, etc.

Multi-Purpose Detector

Stage-I → start of commissioning in 2025

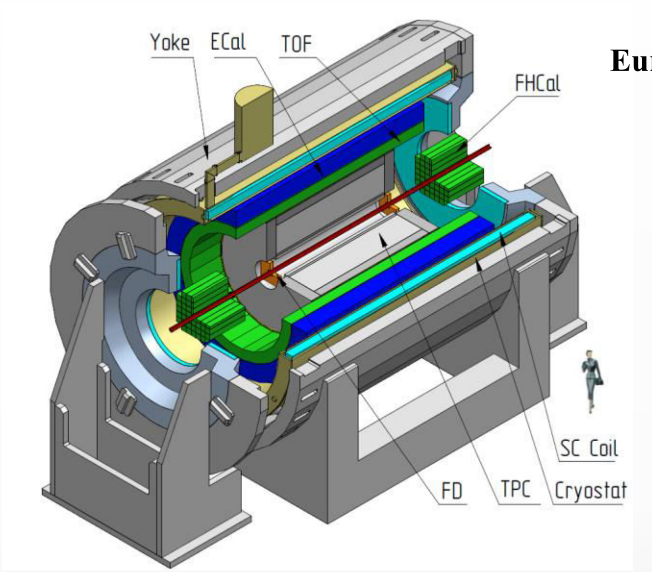

Eur.Phys.J.A 58 (2022) 7, 140

Stage-II → 2030+

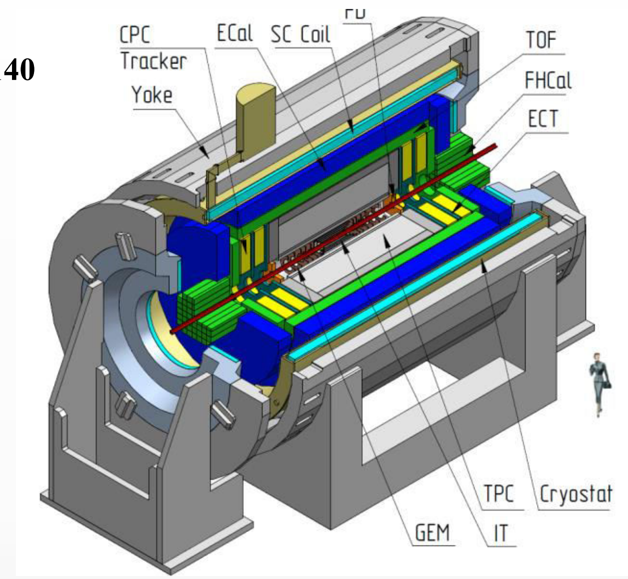

TPC: $|\Delta\varphi| < 2\pi$, $|\eta| \leq 1.6$; **TOF, EMC**: $|\Delta\varphi| < 2\pi$, $|\eta| \leq 1.4$
FFD: $|\Delta\varphi| < 2\pi$, $2.9 < |\eta| < 3.3$; **FHCAL**: $|\Delta\varphi| < 2\pi$, $2 < |\eta| < 5$

+ **ITS** : $|\Delta\varphi| < 2\pi$, $|\eta| \leq 3$
+ **Forward Spectrometers**: $|\Delta\varphi| < 2\pi$, $|\eta| \leq 2.2$

Au+Au @ 11 GeV (full event simulation and reconstruction)

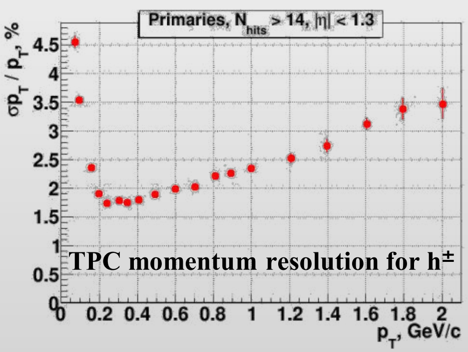

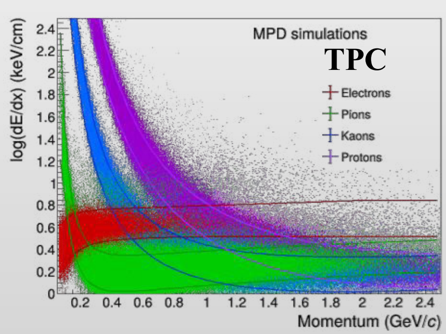

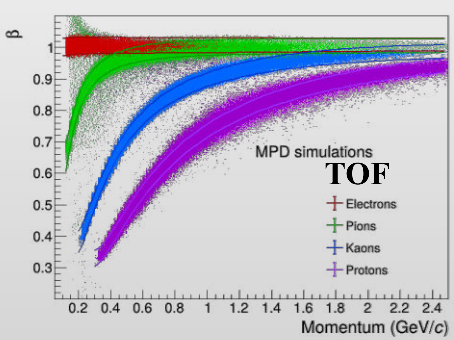

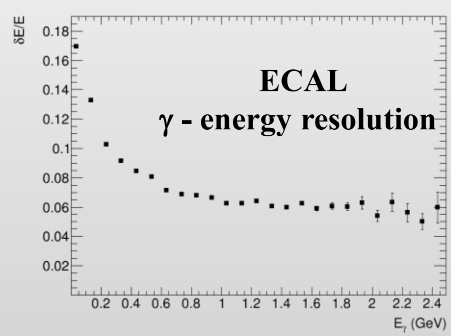

CLD and FXT operation at NICA

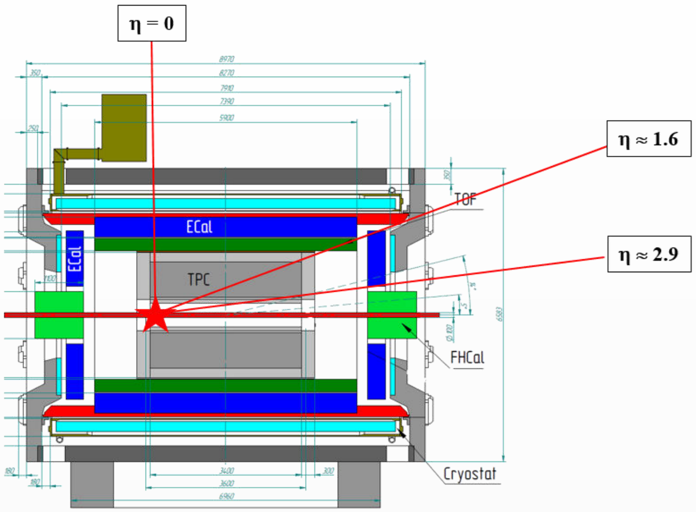

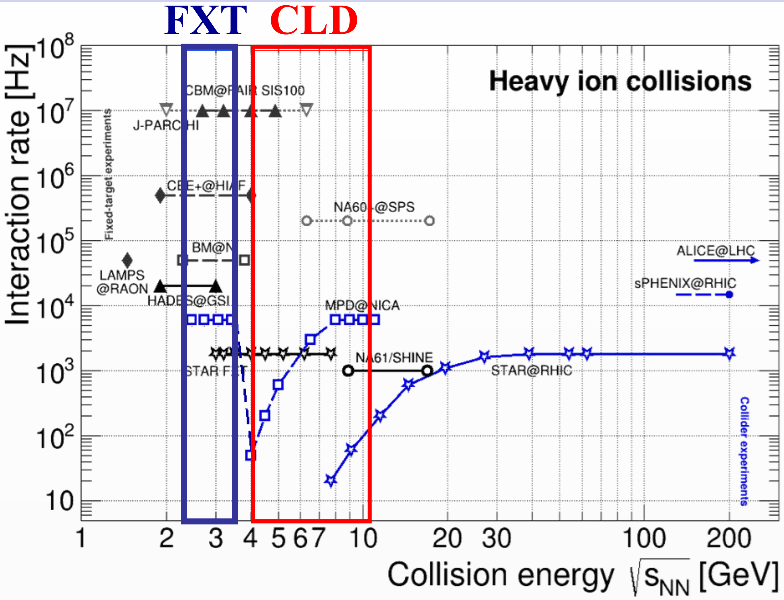

- ❖ MPD-CLD and MPD-FXT operation options
- ❖ Collider mode: two beams, $\sqrt{s_{NN}}$ = 4-11 GeV → Xe+Xe/Bi+Bi at $\sqrt{s_{NN}}$ ~ 7 GeV, ~ 50 Hz at start-up
- ❖ Fixed-target mode: one beam + thin wire (~ 50 μm) → Xe/Bi+W/Au at $\sqrt{s_{NN}}$ ~ 3 GeV, ~ kHz at start-up

- ❖ MPD strategy − high-luminosity scans in **energy** and **system size** to measure a wide variety of signals:
  - ✓ order of the phase transition and search for the QCD critical point → structure of the QCD phase diagram
  - ✓ hypernuclei and equation of state at high baryon densities → inner structure of compact stars, star mergers
- ❖ Scans to be carried out using the **same apparatus** with all the advantages of collider experiments:
  - ✓ maximum phase space, minimally biased acceptance, free of target parasitic effects
  - ✓ correlated systematic effects for different systems and energies → simplified extraction of physical signals

Trigger detectors

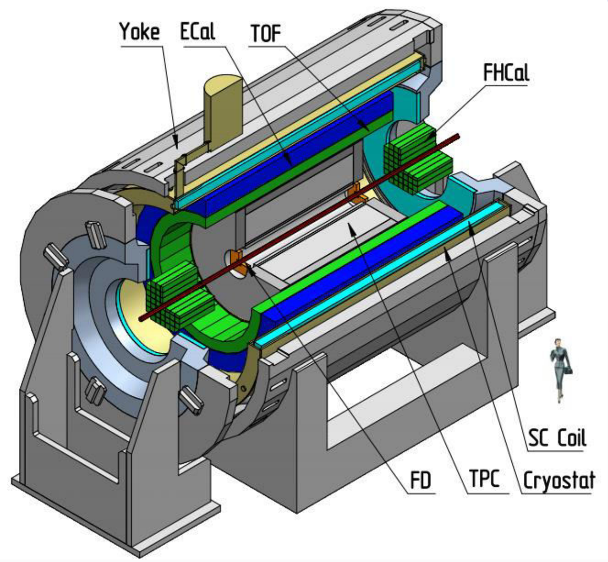

- FFD (Fast Forward Cherenkov Detector):
  - ✓ fast (~ 50 ps) event triggering → photons from π^0's
  - ✓ T_0 for time-of-flight measurements (TOF and ECAL)

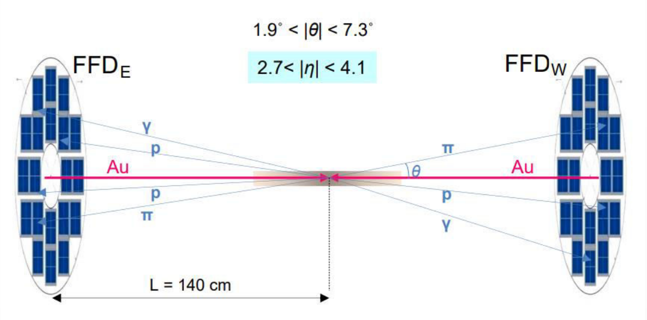

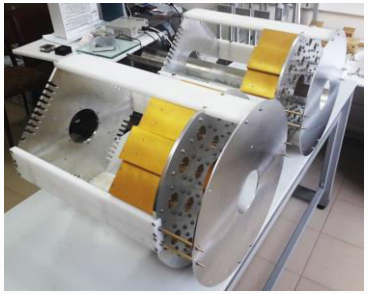

- TOF ($|\eta| < 1.5$):
  - ✓ 280 fast signals for each MRPC chamber
  - ✓ no online timing information

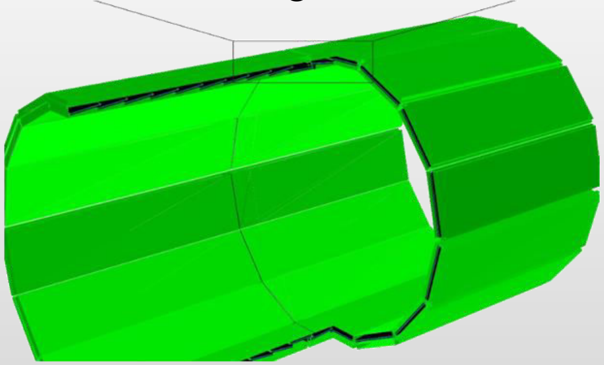

- FHCAL (Forward Hadron Calorimeter):
  - ✓ Fast signals for event triggering
  - ✓ poor T_0 (~ 1 ns) and event z-vertex resolution

two FHCAL detectors
at $2 < |\eta| < 5$,
~ 1x1 m^2 each

Trigger system of the MPD is effective for <u>different HI collision systems and energies</u> as well as for <u>different operation modes</u> (MPD-CLD vs. MPD-FXT)

MPD magnet

Magnet yoke

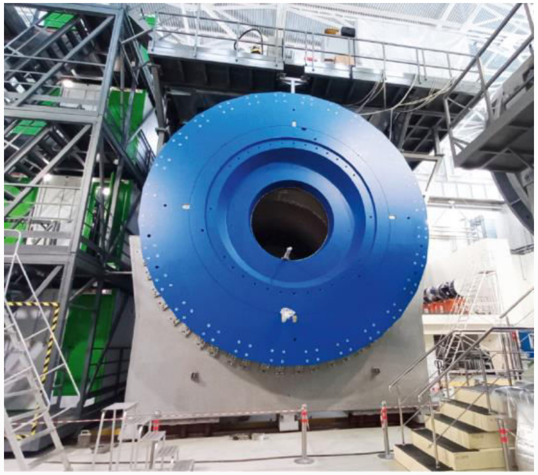

Cryogenic platform

Strings for cryogenic pipes and cables hold

- February: solenoid power cable thermal isolation inside of the Chimney
- Now: solenoid cooled down to the working temperature of 4.5 K, test current supply

Magnetic field mapper

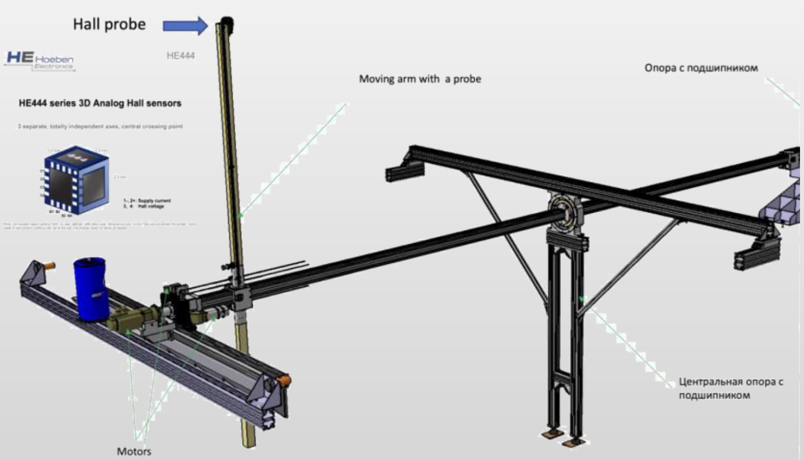

Novosibirsk BINP magnetic field mapper

	Along radius (R)	Along azimuth angle (ϕ)	Along beam (z)
Step size, см	5	21	10
Total length, см	220	360° (1380 см at max. R)	700
Number of measurements	44	64	70

Single 3D Hall probe moves in 3 directions: z , R, ϕ
Accuracy: 0.1 – 0.3 Gs
Number of points: ~ $2{\cdot}10^5$ (90 hours)
Fields to measure: 0.3 – 0.57 T (5-6 points)
Number of tunes per field: 5
Total time of measurements: ~ 3-4 months

April: mapper delivery to JINR and installation of stationary Hall probes
Summer: MF measurements at 02-0.55 T

Central barrel subsystems

Frame - ready

Carbon fiber support frame delivered and unpacked, sagita ~ 5 mm at full load, rails for the TPC and TOF are installed

ECAL

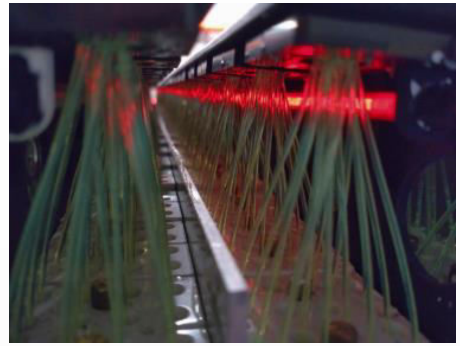

ECAL ~ 38400 towers (2400 modules)
produced by Tsinghua University, Shandong University, Fudan University, South China University, Huzhou University and JINR – production in IHEP (Protvino) and Tenzor (Dubna)

45 half-sectors to be ready by August, the rest depends on WLS fiber supply from Tver

TOF - ready

All 28 (100%) TOF modules are assembled, tested, stored and ready for installation. Spare modules in production

TPC – central tracking detector

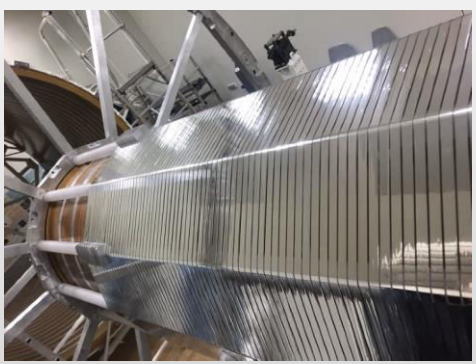

24+ ROC ready; 100+ % FE cards manufactured
TPC gas volume assembly and HV/leakage tests – ongoing
TPC + ECAL cooling systems under commissioning

TPC mechanical body assembly with ROCs, leak test and HV test	**June 2025**
TPC installation to MPD and test	**Nov –Dec 2025**

Starting detector commissioning in late 2025 remains the main priority

MPD physics program

❖ A comprehensive physics program: ions from **p** to **Au** and collision energies $\sqrt{s_{NN}}$= 2.4-11 GeV

G. Feofilov, P. Parfenov

Global observables

- Total event multiplicity
- Total event energy
- Centrality determination
- Total cross-section measurement
- Event plane measurement at all rapidities
- Spectator measurement

V. Kolesnikov, Xianglei Zhu

Spectra of light flavor and hypernuclei

- Light flavor spectra
- Hyperons and hypernuclei
- Total particle yields and yield ratios
- Kinematic and chemical properties of the event
- Mapping QCD Phase Diag.

K. Mikhailov, A. Taranenko

Correlations and Fluctuations

- Collective flow for hadrons
- Vorticity, Λ polarization
- E-by-E fluctuation of multiplicity, momentum and conserved quantities
- Femtoscopy
- Forward-Backward corr.
- Jet-like correlations

D. Peresunko, Chi Yang

Electromagnetic probes

- Electromagnetic calorimeter meas.
- Photons in ECAL and central barrel
- Low mass dilepton spectra in-medium modification of resonances and intermediate mass region

Wangmei Zha, A. Zinchenko

Heavy flavor

- Study of open charm production
- Charmonium with ECAL and central barrel
- Charmed meson through secondary vertices in ITS and HF electrons
- Explore production at charm threshold

Collaboration papers

- Collaboration papers:

  I. **Status and initial physics performance studies of the MPD experiment at NICA**
  Eur.Phys.J.A 58 (2022) 7, 140 (~ 50 pages)

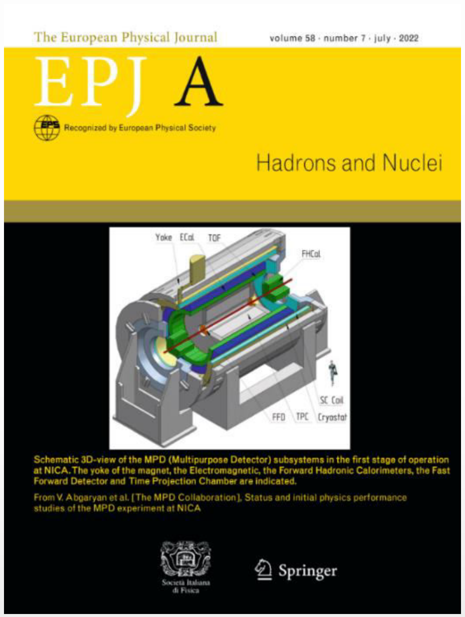

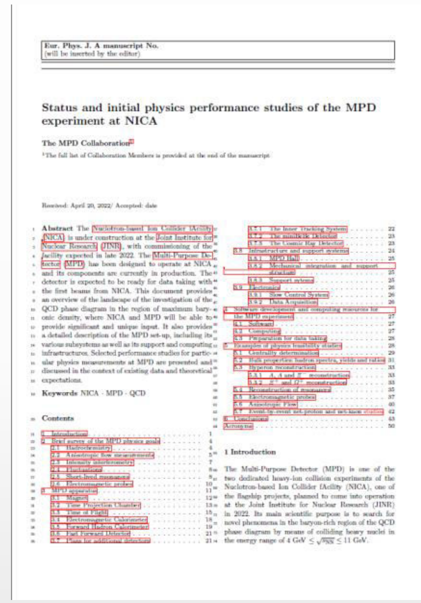

  II. **MPD physics performance studies in Bi+Bi collisions at $\sqrt{s_{NN}}$ = 9.2 GeV**
  consolidation and publication of physics feasibility studies for BiBi@9.2 GeV, 40+ pages

arXiv:2503.21117 [nucl-ex]

paper has been submitted to the journal, Revista Mexicana de Física

Light identified hadrons

- ✓ probe freeze-out conditions
- ✓ radial flow and collective expansion
- ✓ hadronization mechanisms, thermal models vs. coalescence
- ✓ strangeness production, "horn" for K/π, hidden strangeness with $\phi(1020)$
- ✓ lifetime and properties of the late hadronic phase
- ✓ fluctuation of net-baryon (proton) and net-strangeness (kaon) numbers
- ✓ parton energy loss
- ✓ …

Charged hadrons, Bi + Bi @ 9.2 GeV

- Charged hadrons: large and uniform acceptance + excellent PID capabilities of TPC and TOF

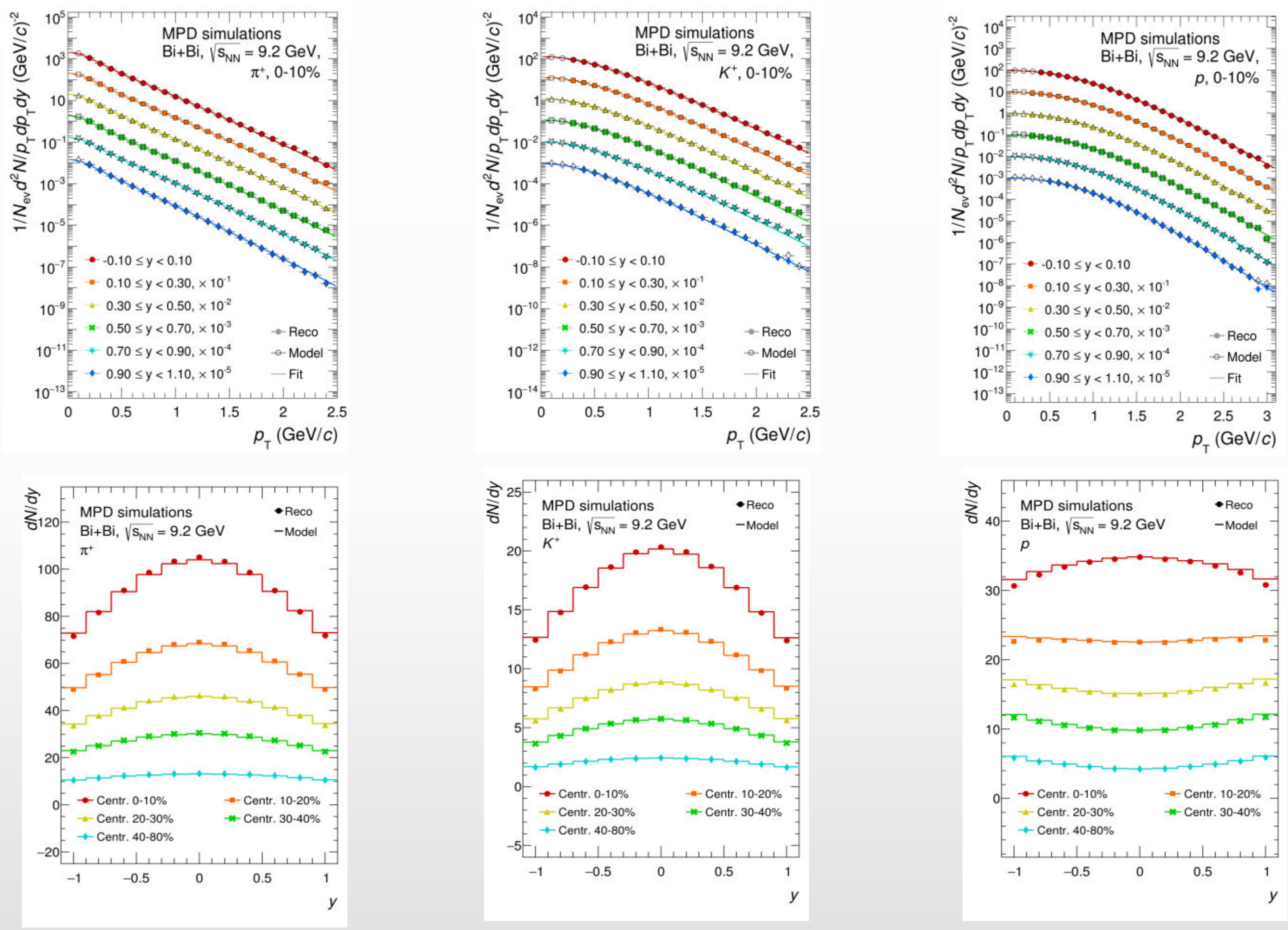

Cover (p_T - rapidity) phase space corresponding to ~ 70% of π/K/p total production

Cover p_T range that corresponds to > 90% of π/K/p total production at midrapidity → small unc. for dN/dy

Wide p_T coverage for combined Blast-Wave fits → β, T_{kin}

Neutral identified hadrons, Bi + Bi @ 9.2 GeV

- Neutral mesons:
  - ✓ $\pi^0/\eta \to \gamma\gamma$, $\pi^0/\eta \to \gamma(e^+e^-)$, $\pi^0/\eta \to (e^+e^-)(e^+e^-)$; $K_s \to \pi^0\pi^0$; $\omega \to \pi^0\gamma$, $\omega/\eta \to \pi^0\pi^+\pi^-$; $\eta' \to \eta\pi^+\pi^-$
- Photons: ECAL reconstruction + photon conversion method (PCM)

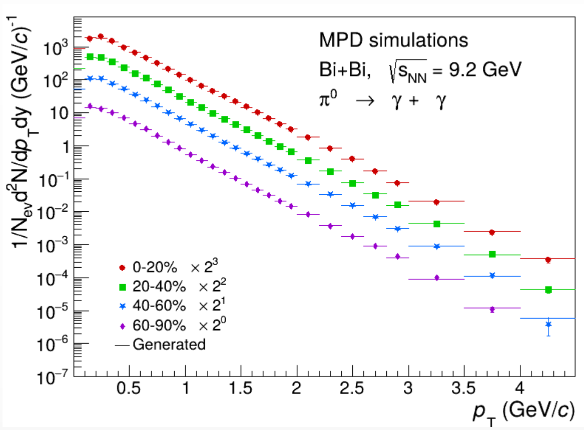

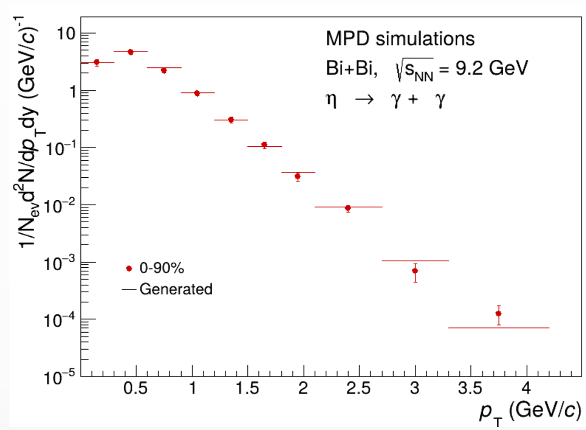

Extended p_T ranges compared to charged particle measurements

Different systematics and species (masses, quark contents)

- … and event baryons: $\Sigma^0 \to \Lambda\gamma$, $\Sigma^0 \to \Lambda(e^+e^-)$, $\Sigma^+ \to p\pi^0$

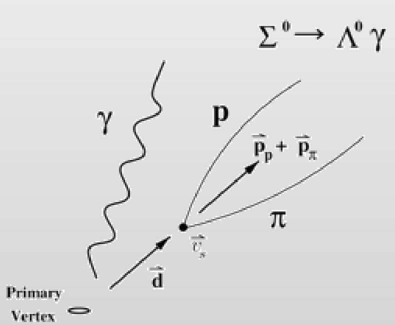

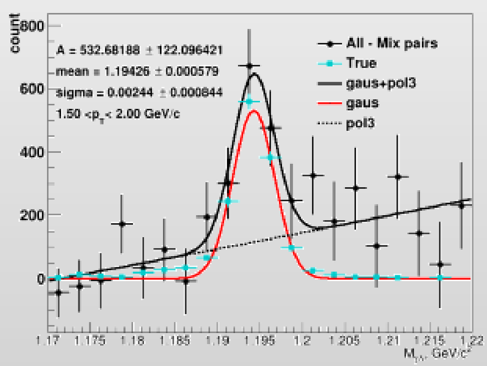

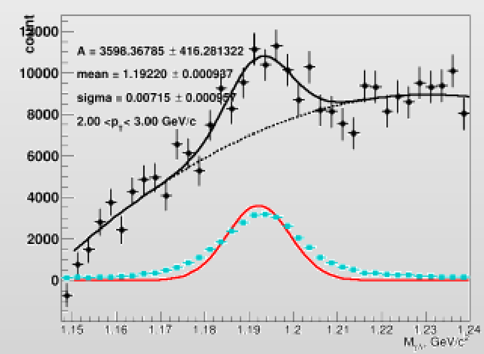

Hadronic resonances

- Resonances probe reaction dynamics and particle production mechanisms vs. system size and $\sqrt{s_{NN}}$:
  - ✓ strangeness production, lifetime and properties of the hadronic phase, spin alignment of vector mesons, flow etc.

increasing lifetime ⟶

	$\rho(770)$	$K^*(892)$	$\Sigma(1385)$	$\Lambda(1520)$	$\Xi(1530)$	$\phi(1020)$
$c\tau$ (fm/c)	1.3	4.2	5.5	12.7	21.7	46.2
$\sigma_{rescatt}$	$\sigma_\pi\sigma_\pi$	$\sigma_\pi\sigma_K$	$\sigma_\pi\sigma_\Lambda$	$\sigma_K\sigma_p$	$\sigma_\pi\sigma_\Xi$	$\sigma_K\sigma_K$

- Properties of the hadronic phase are studied by measuring ratios of resonance yields to yields of long-lived particles with same/similar quark contents: ρ/π, K^*/K, ϕ/K, Λ^*/Λ, $\Sigma^{*\pm}/\Sigma$ and Ξ^{*0}/Ξ

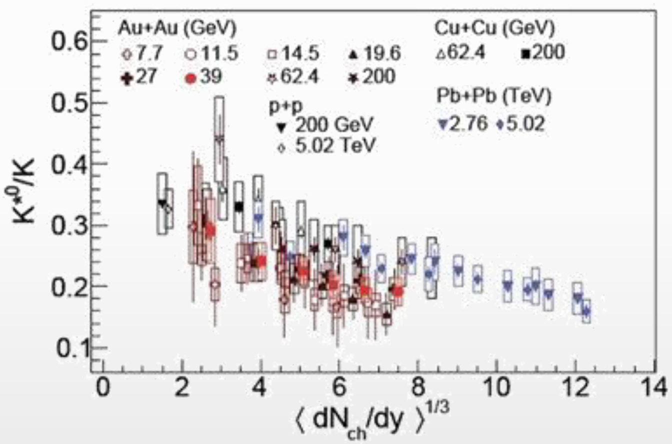

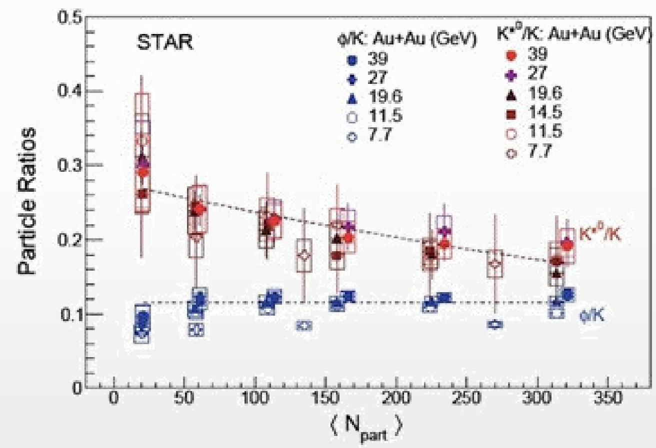

- Suppression of the ratios for shorter-lived resonances is explained by the existence of a <u>hadronic phase that lives long enough (up to τ ~ 10 fm/*c*)</u> to cause a significant reduction of the reconstructed yields → present at NICA confirmed by measurements and transport model (UrQMD) calculations

Precise measurements at NICA are needed to validate description of the hadronic phase in models

Hadronic resonances, Bi + Bi @ 9.2 GeV

- ❖ PID capabilities of TPC and TOF + topology selections for weak decays of daughters (K_s, Λ)

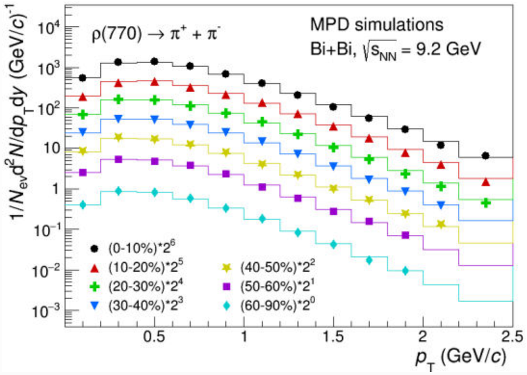

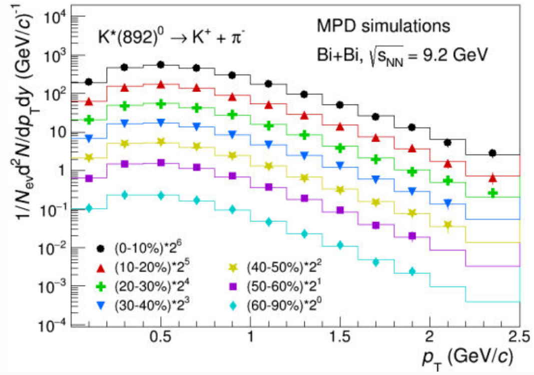

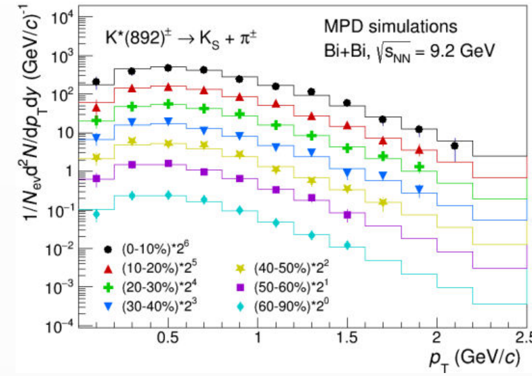

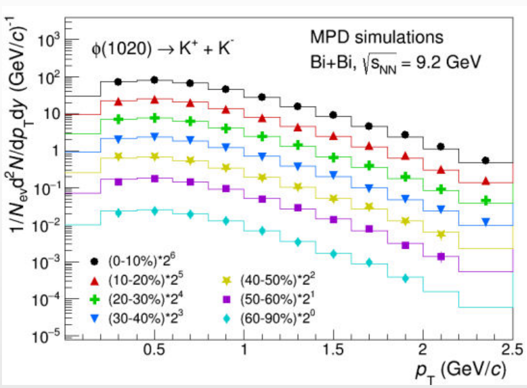

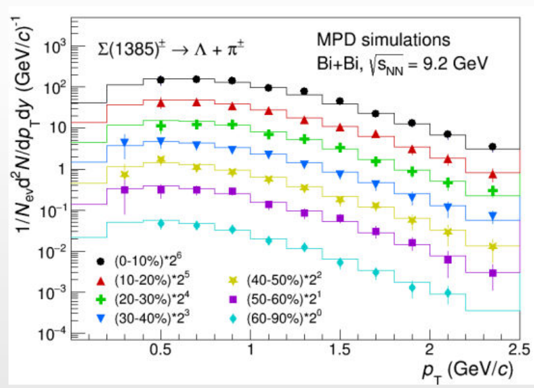

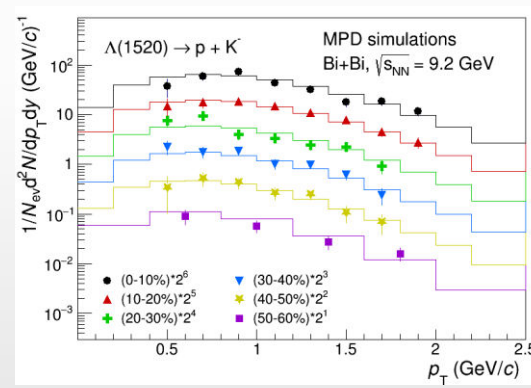

A wide variety of resonances is constructible, ρ(770), K*(892), ϕ(1020), Σ(1385), Λ(1520)

Measurements are possible starting from ~ zero momentum → sample most of the yields

Angular dependent measurements with larger statistics → spin alignment, collective flow

(Multi)strange baryons

Strangeness production

- Small hadronic cross-sections
  → sensitivity to early stages of medium dynamics

- Yields of strange hadrons (low p_T)
  → strangeness enhancement, proposed as a signature of QGP since 80's, now described by statistical/thermal models
  → information about chemical freeze-out parameters
  → near or sub-threshold production

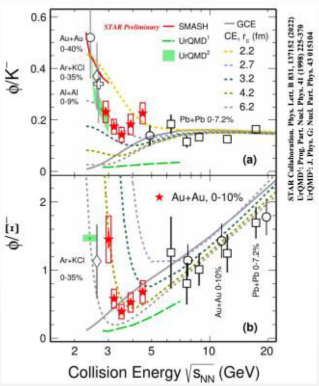

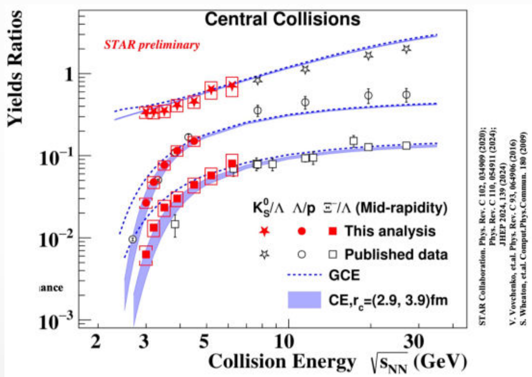

$$\ln(\overline{B}/B) = -2\mu_B/T_{ch} + \mu_S/T_{ch}\Delta S$$

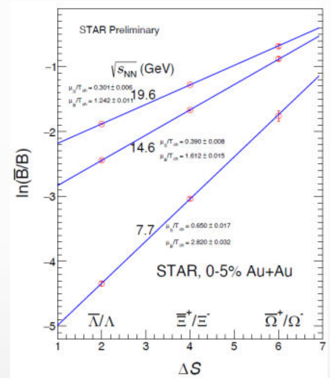

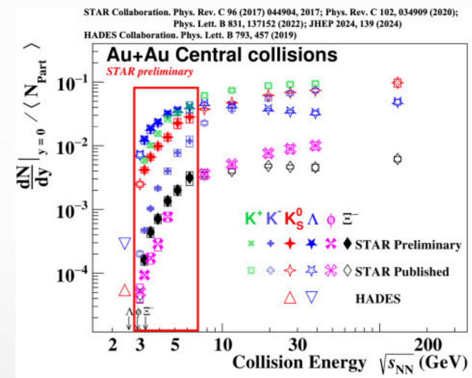

- Hyperon-to-meson ratios vs. p_T (intermediate p_T)
  → hadronization with parton coalescence, freeze-out conditions

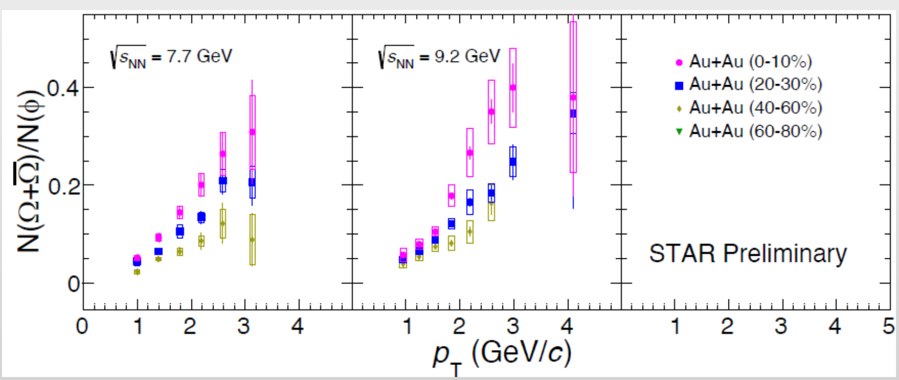

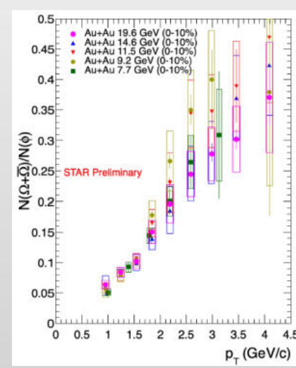

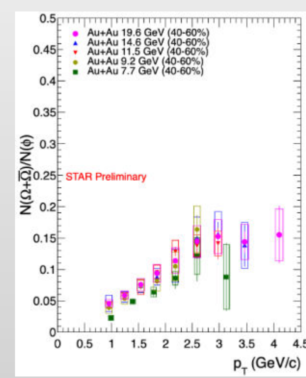

Hyperons, Bi + Bi @ 9.2 GeV

❖ PID capabilities of TPC and TOF + topology selections

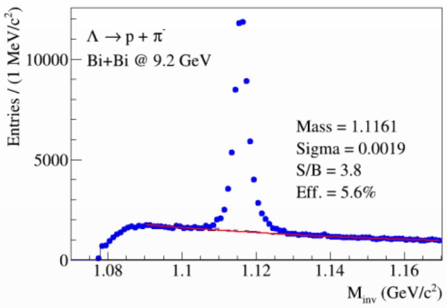

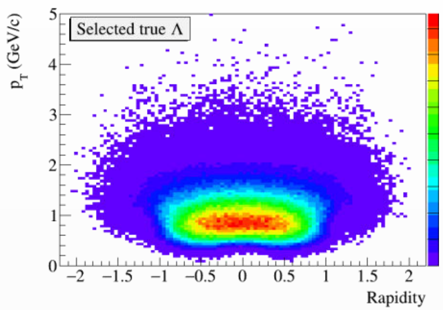

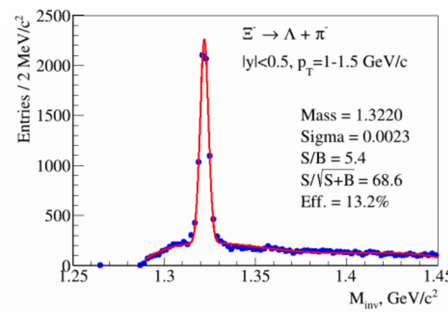

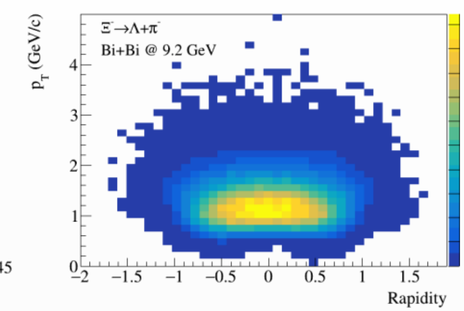

- different background estimates (fit function vs mixed-event), testing alternative Machine Learning techniques

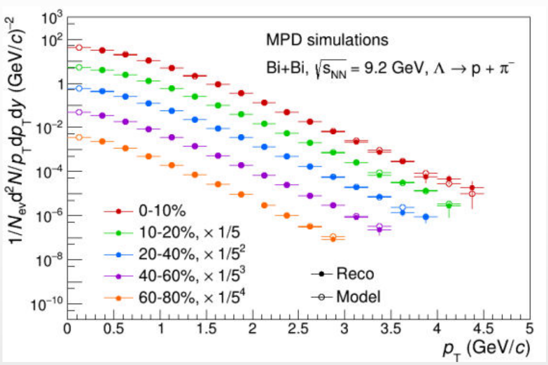

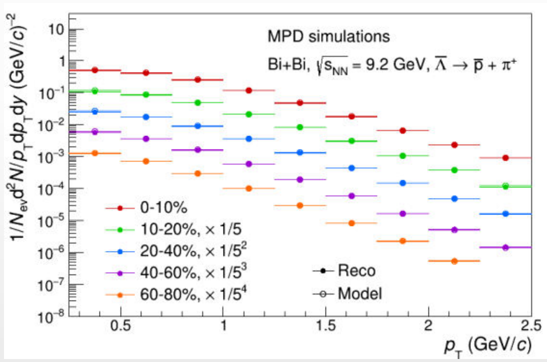

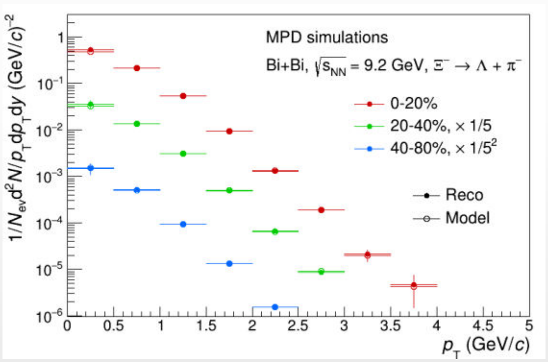

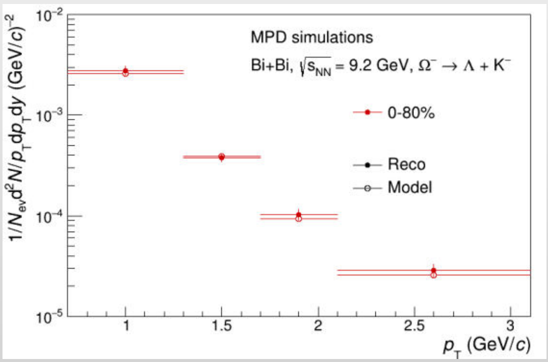

MPD has capabilities to measure production of strange charged/neutral kaons, (multi)strange baryons and resonances in pp, p-A and A-A collisions using h-ID in the TPC&TOF and different decay topology selections

Hyperon global polarization

- Global polarization of hyperons experimentally observed, decreases with $\sqrt{s_{NN}}$

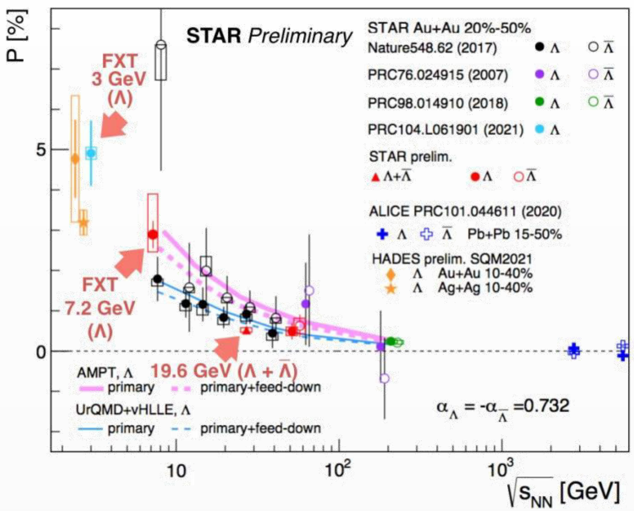

- ✓ reproduced by AMPT, 3FD, UrQMD+vHLLE
- ✓ hint for a Λ-$\bar{\Lambda}$ difference, magnetic field: ,

$$P_\Lambda \simeq \frac{1}{2}\frac{\omega}{T} + \frac{\mu_\Lambda B}{T} \qquad P_{\bar{\Lambda}} \simeq \frac{1}{2}\frac{\omega}{T} - \frac{\mu_\Lambda B}{T}$$

NICA: <u>extra points in the energy range 2-11 GeV</u>
centrality, p_T and rapidity dependence of polarization,
not only for Λ, but other (anti)hyperons (Λ, Σ, Ξ)

- MPD performance: BiBi@9.2 GeV (PHSD, 15 M events) → full reconstruction → Λ global polarization

Performance study of the hyperon global polarization measurements with MPD at NICA, Eur.Phys.J.A 60 (2024) 4, 85

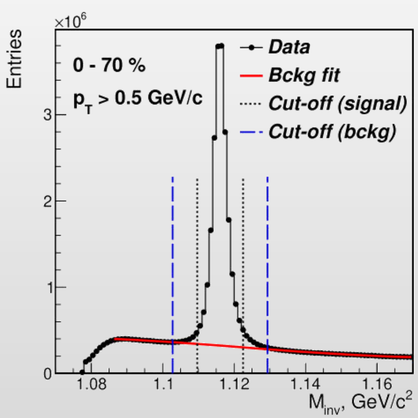

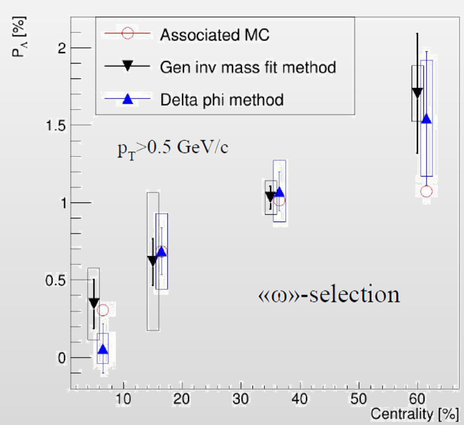

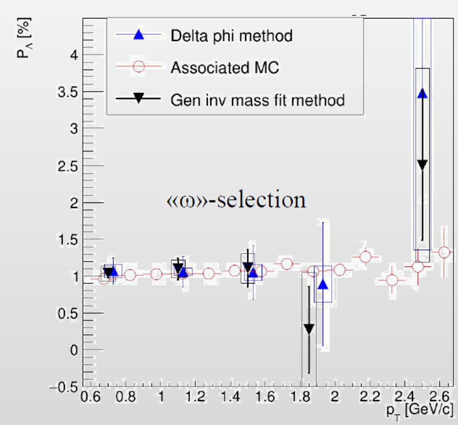

MPD: first global polarization measurements for $\Lambda/\bar{\Lambda}$ will be possible with ~ 20M data sampled events

Light (hyper)nuclei

(Hyper)nuclei

- ❖ Production mechanism usually described with two classes of phenomenological models :
  - ✓ statistical hadronization (SHM) → production during phase transition, dN/dy ∝ exp(-m/T_{chem}) [1]
  - ✓ coalescence → (anti)nucleons close in phase space ($\Delta p < p_0$) and matching the spin state form a nucleus [2]
- ❖ Hyper nuclei measurement studies are crucial:
  - ✓ microscopic production mechanism, Y-N potential, strange sector of nuclear EoS
  - ✓ strong implications for astronuclear physics → hyperons expected to exist in the inner core of neutron stars
- ❖ Models predict enhanced hypernuclear production at NICA energies→ offers great opportunity for hypernuclei measurements in MPD, double hypernuclei may be reachable
- ❖ Observables of interest: binding energies, lifetimes, branching ratios, <p_T>, dN/dy

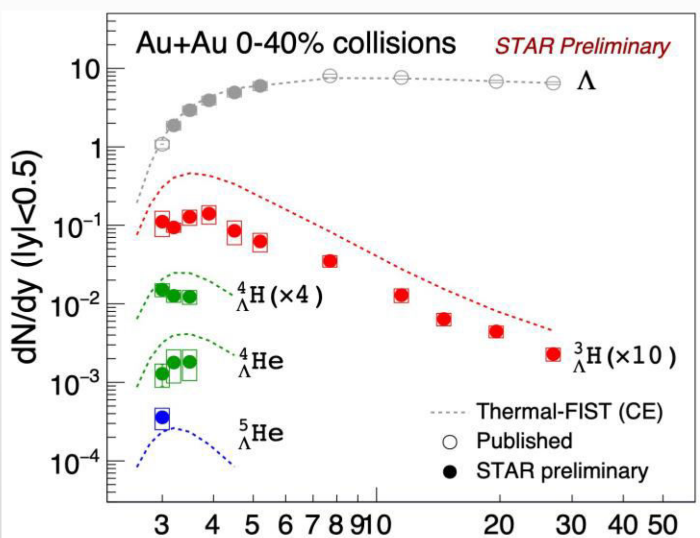

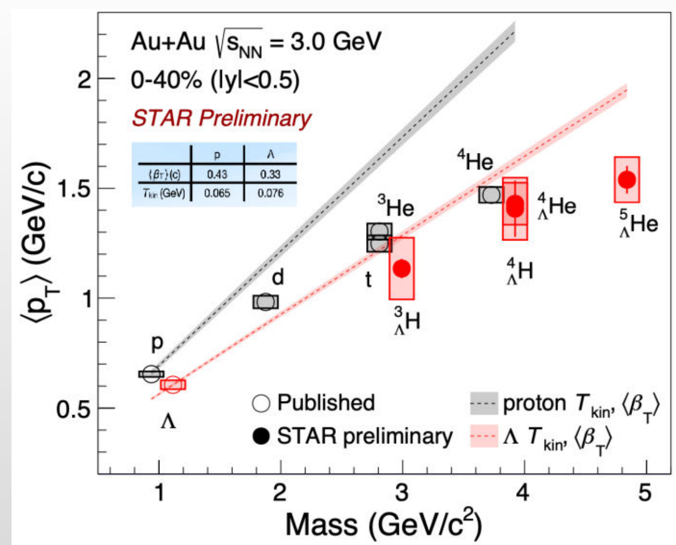

Light nuclei in the MPD

❖ MPD has excellent light fragment identification capabilities in a wide rapidity range

dE/dx vs momentum in TPC

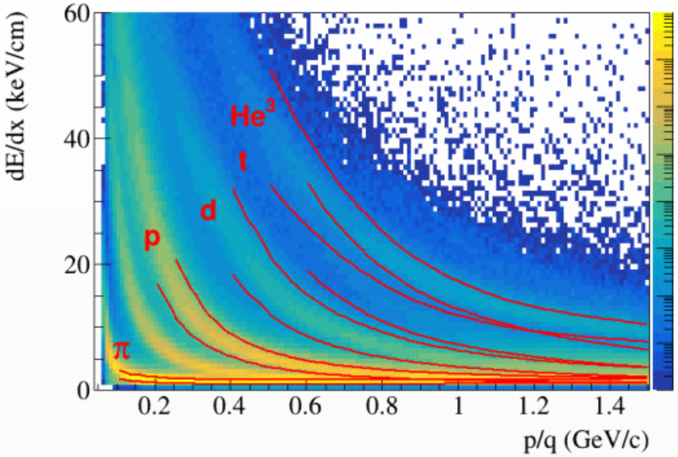

m² vs. momentum in TOF

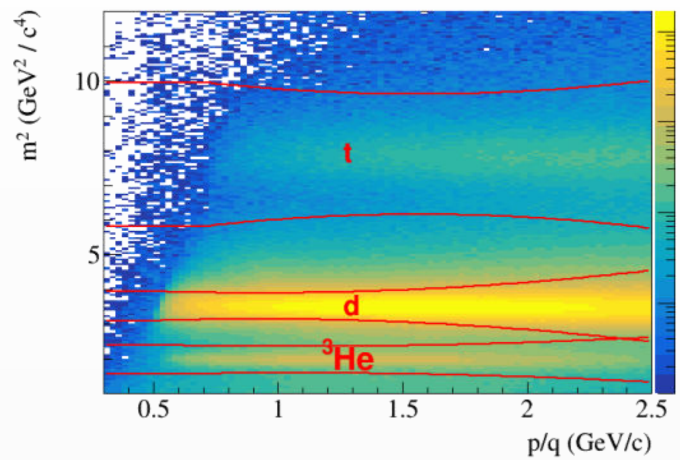

❖ Light nuclei reconstruction, Bi + Bi @ 9.2 GeV (PHQMD)

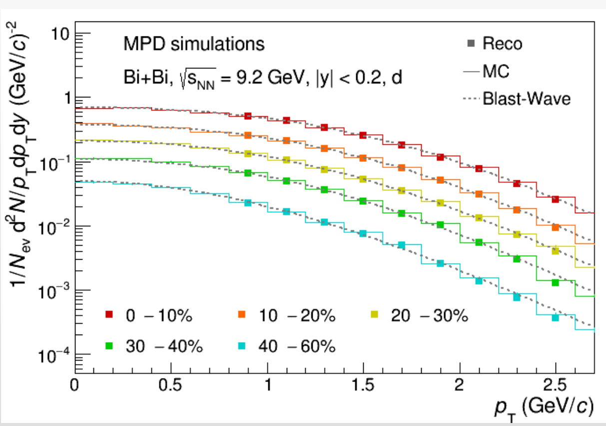

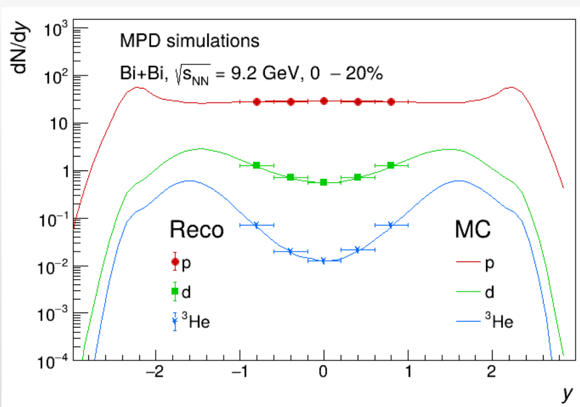

❖ NICA accelerator can deliver different ion beam species and energies → input to the heavy-ion data base for applied and space research to simulate damage from cosmic rays to astronauts, electronics, and spacecraft

MPD performance for hypenuclei

❖ Mass production 29 (PHQMD, BiBi@9.2 GeV, 40M events)

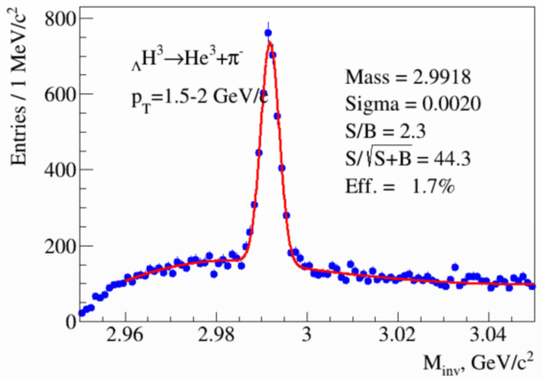

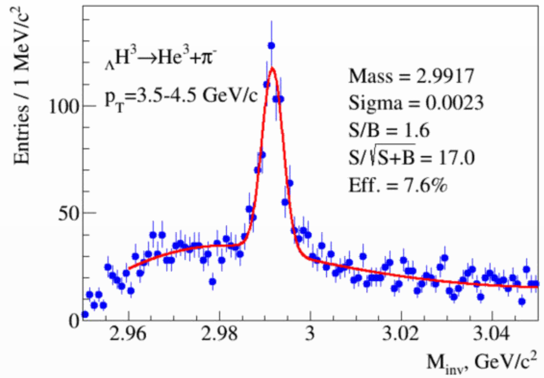

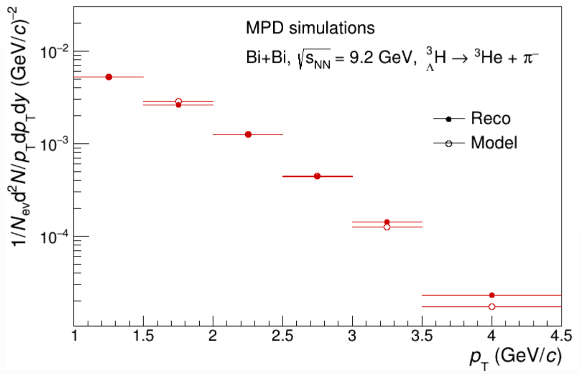

2- and 3-prong decay modes were studied separately to estimate systematics

$$N(\tau) = N(0)\exp\left(-\frac{\tau}{\tau_0}\right) = N(0)\exp\left(-\frac{ML}{cp\tau_0}\right),$$

Decay channel	Branching ratio	Decay channel	Branching ratio
$\pi^- + {}^3He$	24.7%	$\pi^- + p + p + n$	1.5%
$\pi^0 + {}^3H$	12.4%	$\pi^0 + n + n + p$	0.8%
$\pi^- + p + d$	36.7%	$d + n$	0.2%
$\pi^0 + n + d$	18.4%	$p + n + n$	1.5%

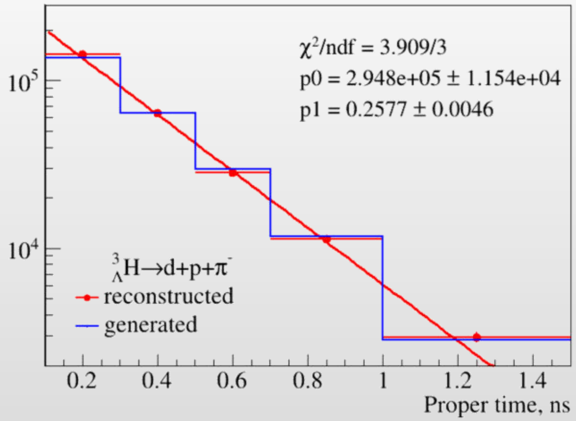

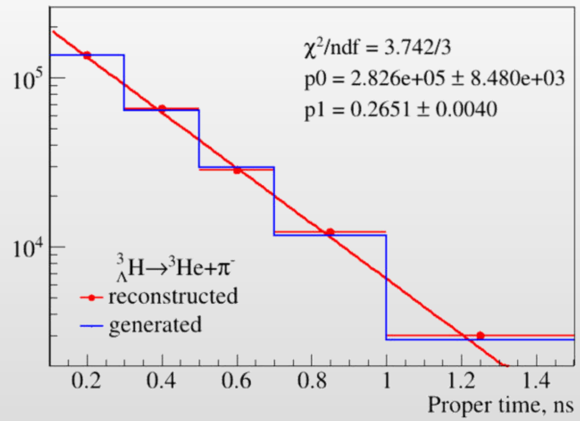

$_\Lambda H^3$ reconstruction with ~ 50M samples events

Heavier hypernuclei

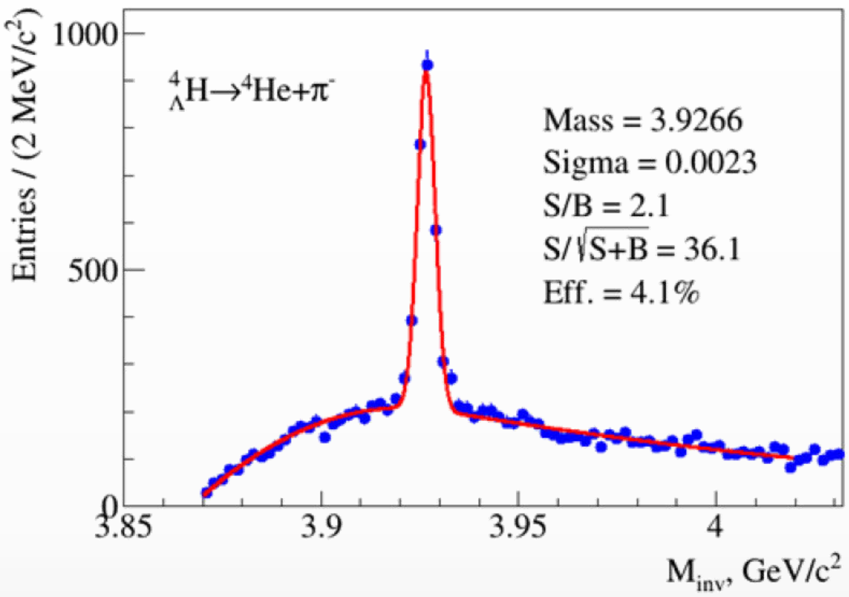

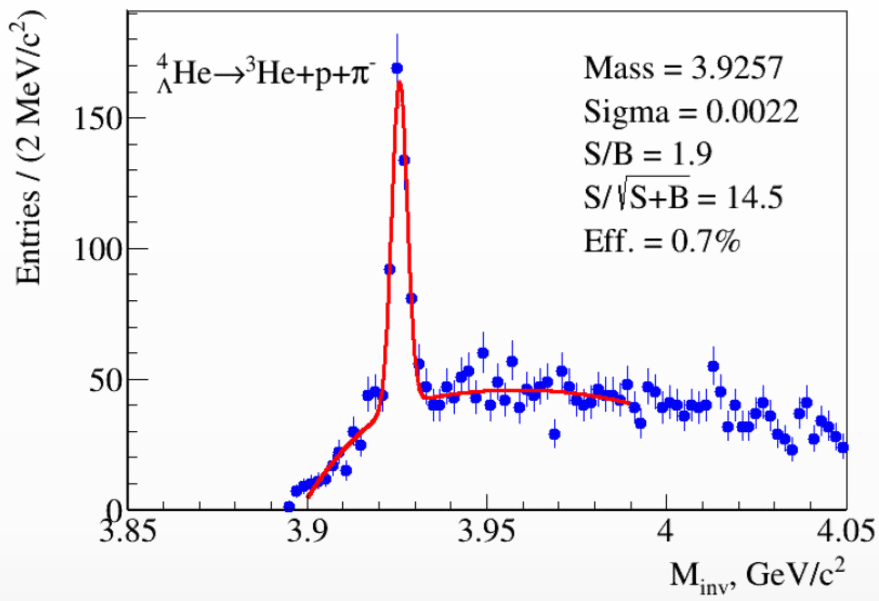

- PHQMD events enhanced with hypernuclei signals with the correct (η-p_T) phase space distribution

$_{\Lambda}H^4$, $_{\Lambda}He^4$ reconstruction with ~ 150M samples events

Initial state

QGP as a relativistic fluid

Electromagnetic radiation

Direct photons and system temperature

- All photons not from the hadron decays:
  - ✓ produced during all stages of the collision → penetrating probe
- Thermal low-E photons → effective temperature of the system:

$$E_\gamma \frac{d^3 N_\gamma}{d^3 p_\gamma} \propto e^{-E_\gamma / T_{\mathrm{eff}}}$$

- Prompt higher-p_T photons:

$$E\frac{d^3\sigma}{dp^3} = \sum_{i,j,k} f_i(x_i, Q^2) \otimes f_j(x_j, Q^2) \otimes D_k(z_k, Q^2) \propto 1/p_T^n$$

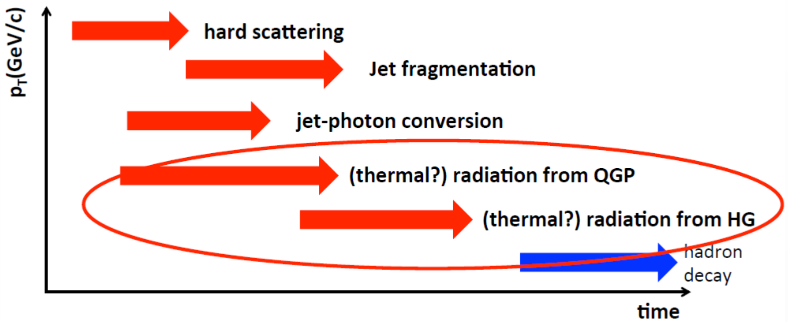

- Relativistic A+A collisions → the highest temperature created in laboratory ~ 10^{12} K

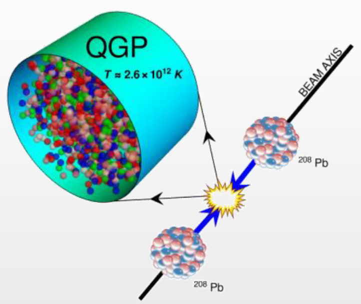

Temperature at the center of the Sun ~ 15 000 000 K

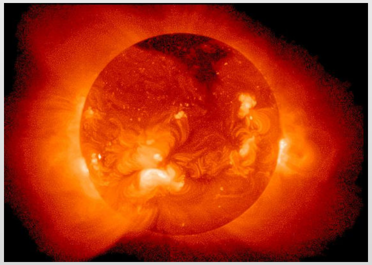

A medium of ~ 200 MeV is 100 000 times hotter !!!

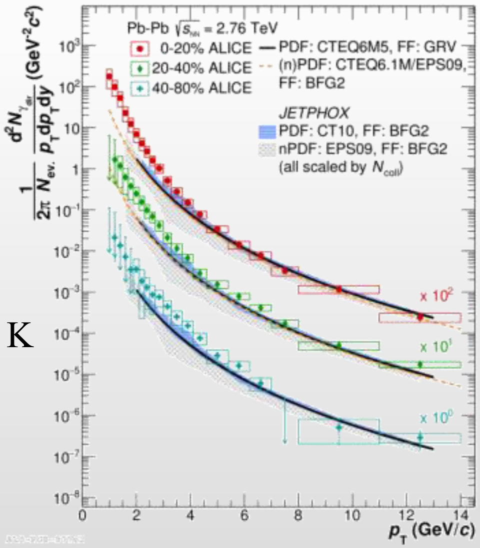

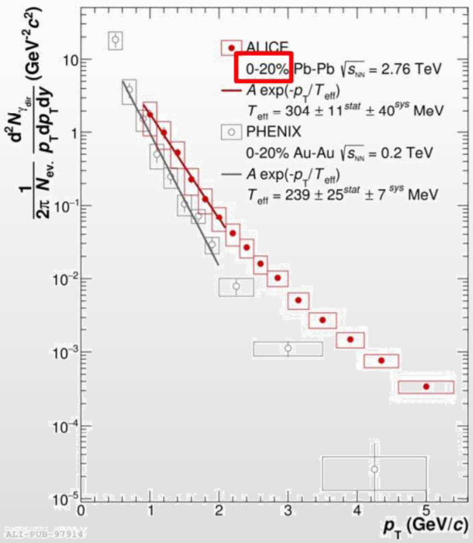

T_{eff} ~ 240 MeV at RHIC; T_{eff} ~ 300 MeV at the LHC

$T_{eff} >> T_c$ ~ 160 MeV predicted by LQCD

Direct photon yields at NICA

Estimation of the direct photon yields @NICA

model calculations

empirical scaling by PHENIX

- ✓ UrQMD v3.4 with hybrid model (3+1D hydro, bag model EoS, hadronic rescattering and resonances within UrQMD)
- ✓ each cell have Ti, Ei, µbi:
  - T is high – QGP phase (Peter Arnold, Guy D. Moore, Laurence G. Yaffe, JHEP 0112:009 2001)
  - T is low – HG phase (Simon Turbide, Ralf Rapp, Charles Gale, Phys.Rev.C69:014903,2004)
  - T is intermediate – mixed phase
- ✓ integrate over all cells and all time steps
- ✓ calculations reproduce hydro calculations for the SPS

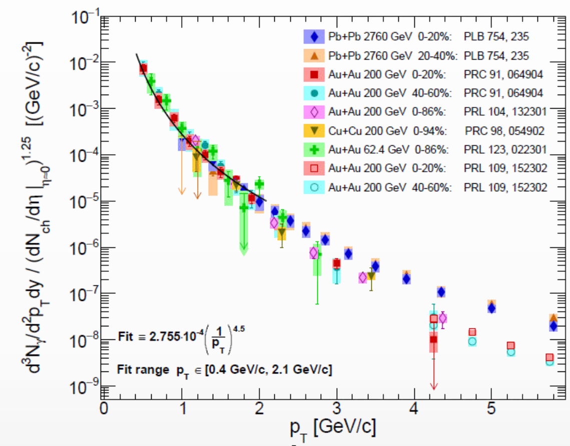

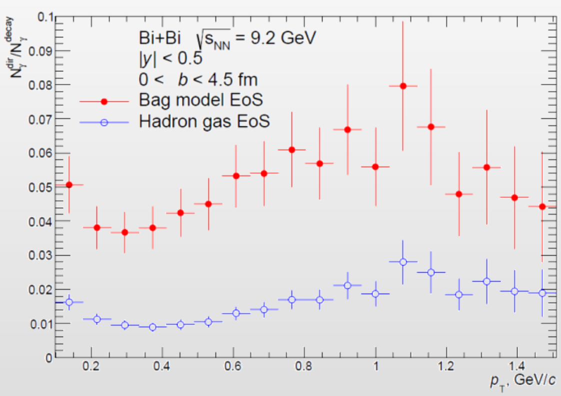

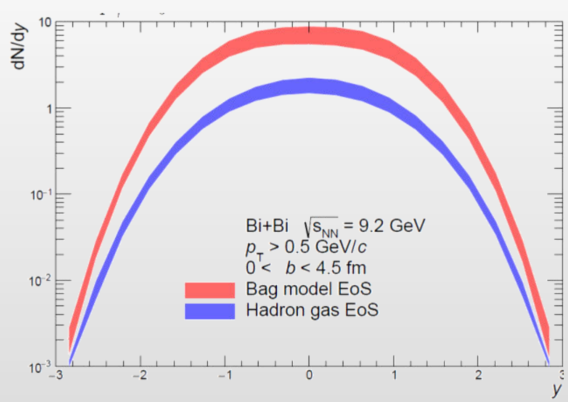

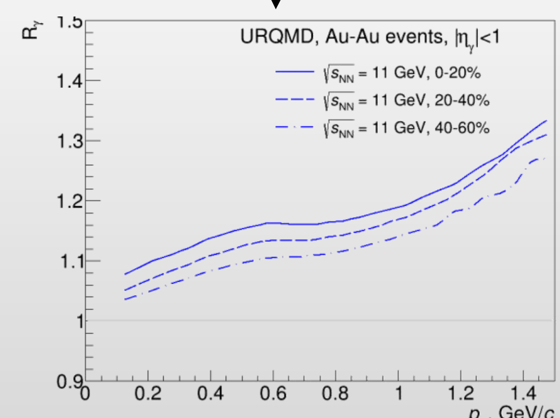

$$R_\gamma = \frac{\gamma_{\text{inc}}}{\gamma_{\text{decay}}} = \frac{\gamma_{\text{inc}}/\pi^0}{\gamma_{\text{decay}}/\pi^0_{\text{param}}}$$

$$\gamma_{\text{direct}} = \left(1 - \frac{1}{R_\gamma}\right)\cdot\gamma_{\text{inc}}$$

❖ Non-zero direct photon yields are predicted with Rγ ~ 1.05 – 1.15 and v2 ~ 0.5% at top NICA energy

Prospects for the MPD

❖ Photons can be measured in the ECAL or in the tracking system as e^+e^- conversion pairs (PCM)

beam pipe (0.3% X_0) + inner TPC vessels (2.4% X_0)

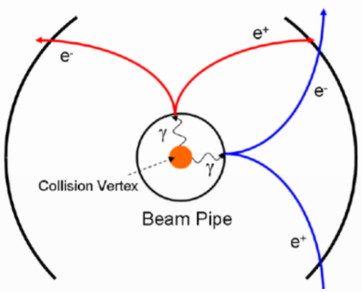

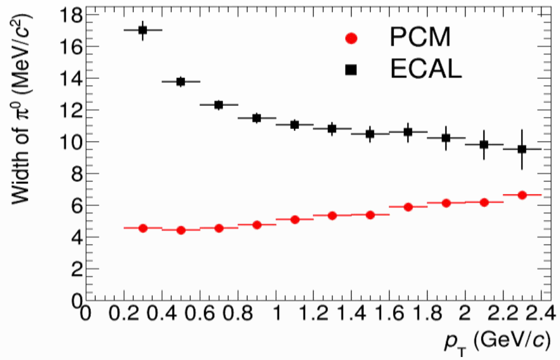

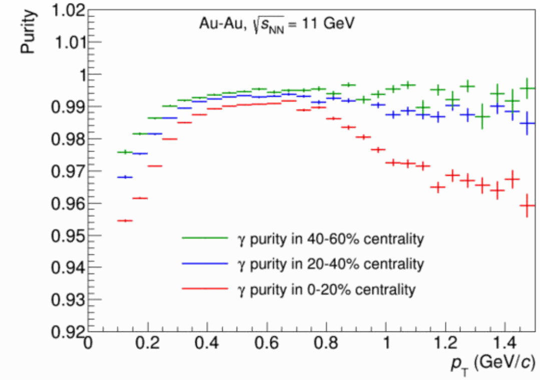

❖ Main sources of systematic uncertainties for direct photons → **potential yield measurements**:

✓ detector material budget → conversion probability; p_T-shapes and reconstruction efficiencies of π^0 and η

✓ with $R\gamma \sim 1.1$ and $\delta R\gamma/R\gamma \sim 3\%$ → uncertainty of $T_{eff} \sim 10\%$

❖ **Measurement of Bose-Einstein correlations** for direct photons:

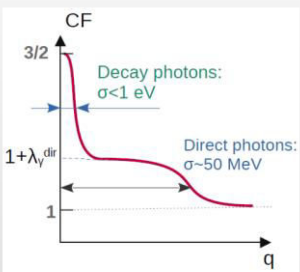

$$C_2(\boldsymbol{q}, \boldsymbol{K}) \approx 1 + \left| \frac{\int d^4x S(x, K)\, e^{iq\cdot x}}{\int d^4x S(x, K)} \right|^2$$

Kinematics variables:

- Relative momentum of the pair: $\boldsymbol{q} = \boldsymbol{p}_1 - \boldsymbol{p}_2$
- Mean pair momentum: $\boldsymbol{K} = \frac{1}{2}(\boldsymbol{p}_1 + \boldsymbol{p}_2)$

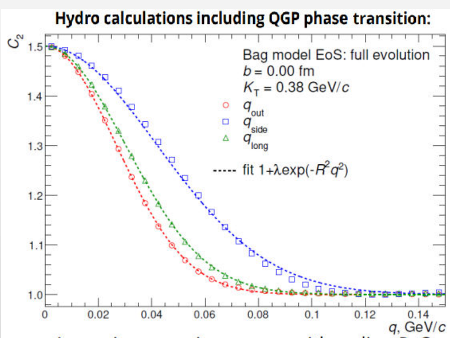

- Assuming gaussian source with radius R, C_2 might be described as

$$C_2(q) = \lambda \exp(-q^2 R^2)$$

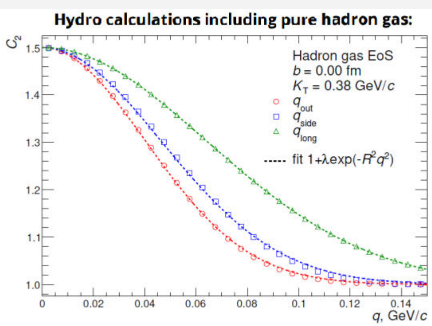

- C_2 are taken at a given mean transverse momentum of a pair

$$K_T = \frac{1}{2}(p_{1T} + p_{2T})$$

✓ Correlation function are different for QGP and HG scenario, the presence of the mixed phase causes increasing of the lifetime

✓ Possibility to extract yields of direct photons at low p_T:

$$\lambda = \frac{1}{2}\left(\frac{N_\gamma^{\mathrm{dir}}}{N_\gamma^{\mathrm{inc}}}\right)^2 \to R_\gamma = \frac{N_\gamma^{\mathrm{inc}}}{N_\gamma^{\mathrm{decay}}} = \frac{1}{1-\sqrt{2\lambda}}$$

MPD can potentially provide measurements for direct photon production in the NICA energy range

Summary

MPD Collaboration meeting in JINR (Dubna): April 23-25

- ❖ NICA energy range → QCD phase diagram at modest temperatures and maximum (net)baryon densities
- ❖ Preparation of the MPD detector and experimental program is ongoing, develop realistic analysis methods and techniques → MPD commissioning with beams in 2025
- ❖ A comprehensive physics program to be studied for different ions (from p to Au) and collision energies ($\sqrt{s_{NN}}$ from 2.4 to 11A GeV), MPD@NICA provides capabilities for important/unique contributions in HIC physics

BACKUP

Polarization of vector mesons: $K^*(892)$ and ϕ

Non-central heavy-ion collisions:

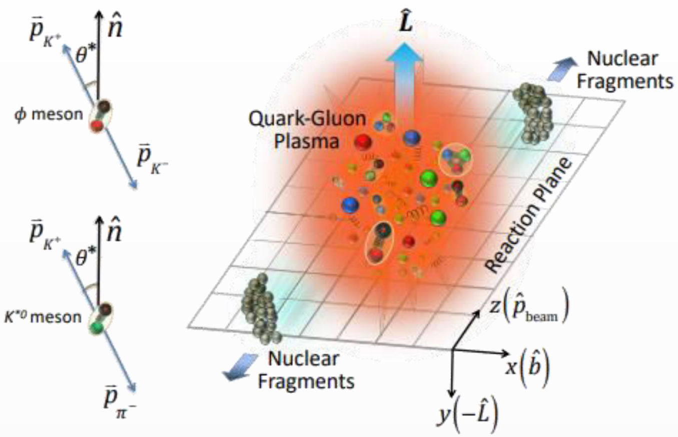

$$\boxed{\frac{dN}{dcos\theta} = N_0[1 - \rho_{0,0} + cos^2\theta(3\rho_{0,0} - 1)]}$$

$\rho_{0,0}$ is a probability for vector meson to be in spin state = 0 $\rightarrow$ $\rho_{0,0}$ = 1/3 corresponds to no spin alignment

The large ρ_{00} puzzle

$$\rho_{00} \approx \frac{1}{3} + C_\Lambda + C_\varepsilon + C_E + C_F + C_L + C_A + C_\varphi + C_g$$

Physics Mechanisms	$\langle\rho_{00}\rangle$
c_Λ: Quark coalescence vorticity & magnetic field[1]	< 1/3 (Negative ~ 10^{-5})
c_ε: E-comp. of Vorticity tensor[1]	< 1/3 (Negative ~ 10^{-4})
c_E: Electric field[2]	> 1/3 (Positive ~ 10^{-5})
c_F: Fragmentation[3]	> or, < 1/3 (~ 10^{-5})
c_L: Local spin alignments[4]	< 1/3
c_A: Turbulent color field[5]	< 1/3
c_φ: Vector meson strong force field[6]	> 1/3 (Can accommodate large positive signal)
c_g: Glasma fields + effective potential	could be significant

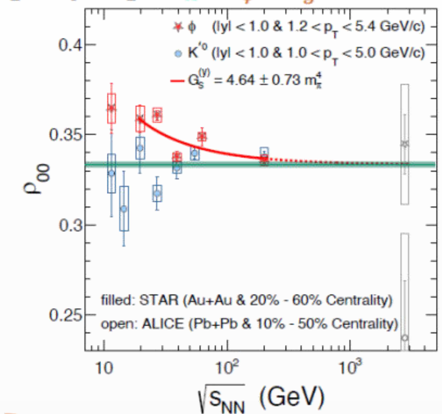

STAR, Nature 614 244 (2023)

strong force

Nature 614 244 (2023)

ϕ exhibits surprisingly large global spin alignment while K* displays little.

Aihong Tang. QuarkMatter 2023, Houston, Sept 3-9 18

- ❖ Measurements at RHIC/LHC challenge theoretical understanding → ρ_{00} can depend on multiple physics mechanisms (vorticity, magnetic field, hadronization scenarios, lifetimes and masses of the particles …)
- ❖ Measurements should be extended to lower collision energies

Nuclear EoS is important also for the r-process nuclear synthesis in neutron star merger

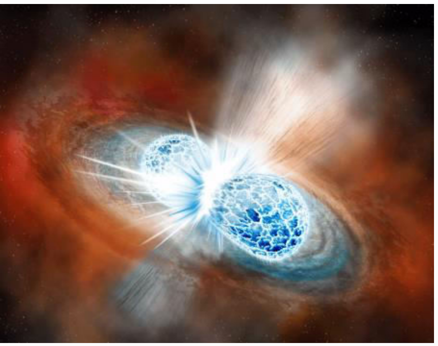

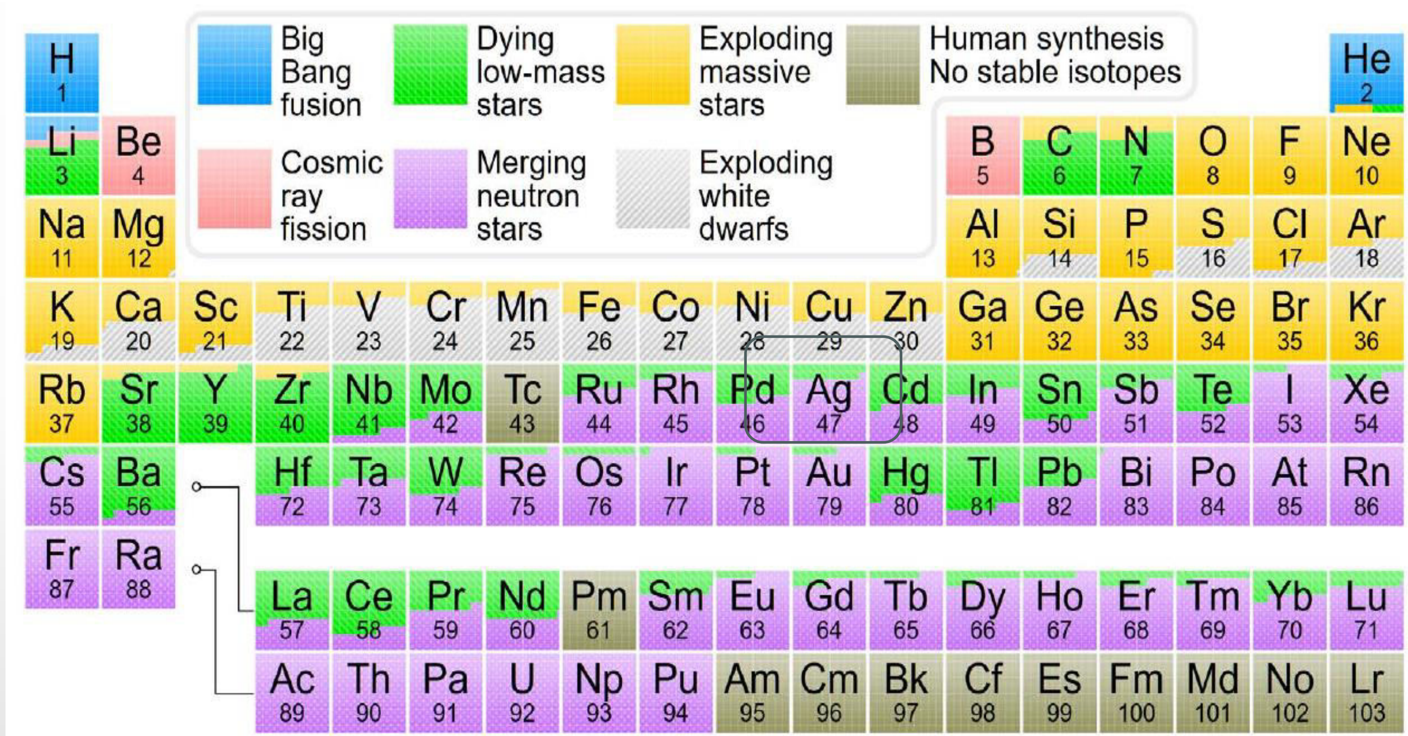

r-process - source of heavy elements including gold, platinum, and uranium.

Collective flow

Collective flow at NICA energies

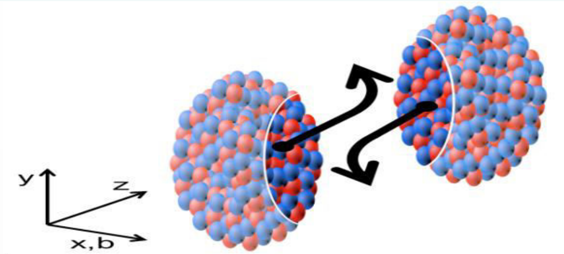

- Generated during the nuclear passage time (2R/γ) – sensitive to EOS
- RHIC @ 200 GeV (2R/γ) ~ 0.1 fm/c
- AGS @ 3-4.5 GeV (2R/γ) ~ 9-5 fm/c
- v_1 and v_2 show strong centrality, energy and species dependence

Phys.Rev.Lett. 112 (2014) 16, 162301

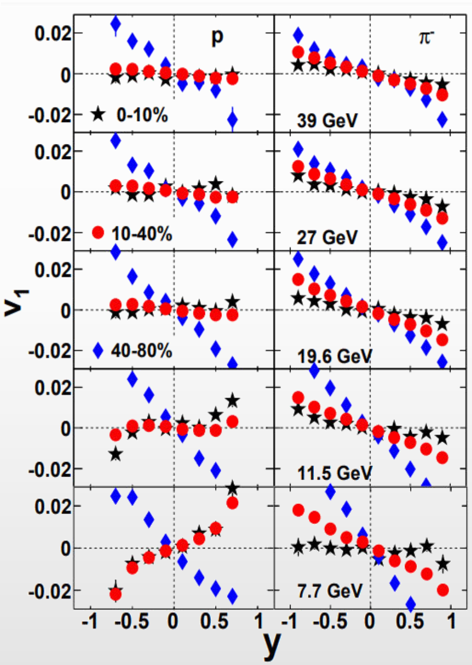

✓ models do not reproduce measurements

EPJ Web Conf. 204 (2019) 03009

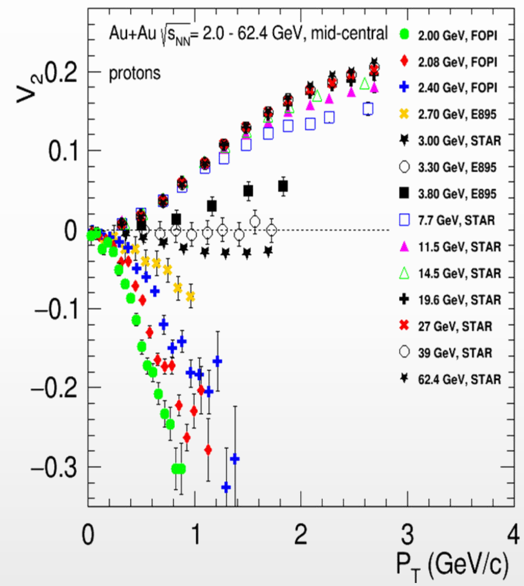

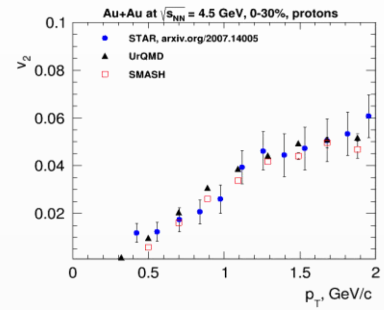

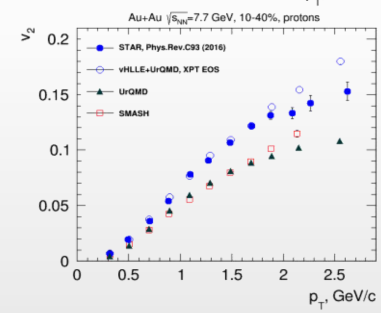

✓ $\sqrt{s_{NN}}$ ~ 3-4.5 GeV, pure hadronic models reproduce v_2 (JAM, UrQMD) → degrees of freedom are the interacting baryons

✓ $\sqrt{s_{NN}} \geq$ 7.7 GeV, need hybrid models with QGP phase (vHLLE+UrQMD, AMPT with string melting,…)

System size scan for flow measurements is vital for understanding of the medium transport properties and onset of the phase transition

Performance for v_1, v_2 of identified hadrons

❖ UrQMD, BiBi@9.2 GeV

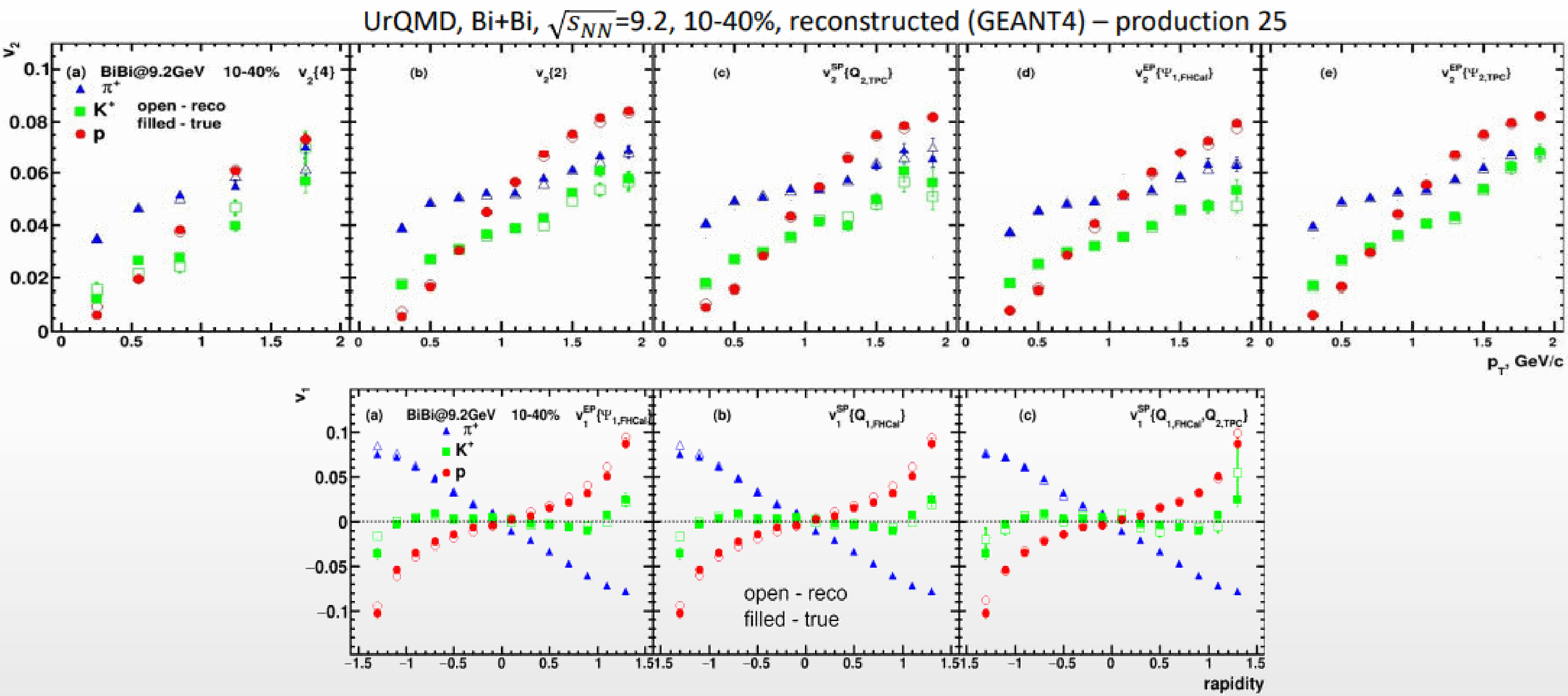

- Reconstructed and generated v_1 and v_2 for identified hadrons are in good agreement for all methods

Anisotropic flow at RHIC/LHC

❖ Initial eccentricity and its fluctuations drive momentum anisotropy v_n with specific viscous modulation

Spatial anisotropy of the nuclear overlap region

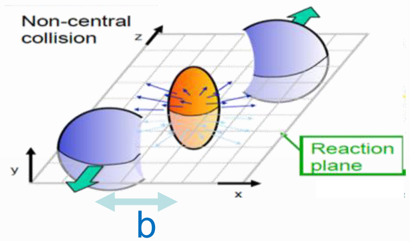

$$\epsilon_n = \sqrt{\frac{\langle r^n \cos n\phi\rangle + \langle r^n \sin n\phi\rangle}{\langle r^n\rangle}}$$

$\epsilon_n \propto v_n$

Azimuthal distribution of produced particles wrt to reaction plane (Ψ_n)

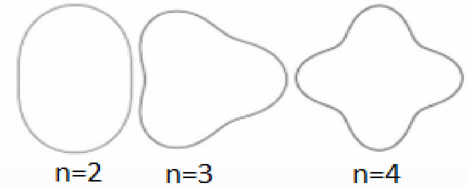

$$\frac{dN}{d\phi} \propto \left(1 + 2\sum_{n=1} v_n \cos\left[n\left(\phi - \Psi_n\right)\right]\right)$$

Anisotropic flow: $v_n = \langle \cos[n(\varphi - \Psi_n)]\rangle$

❖ Evidence for a dense perfect liquid found at RHIC/LHC (M. Roirdan et al., Scientific American, 2006)

Gale, Jeon et al., Phys. Rev. Lett. 110, 012302

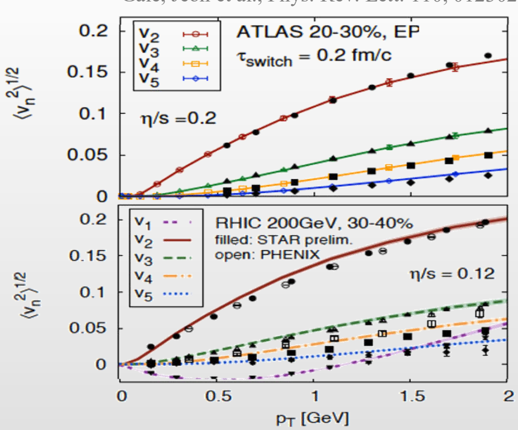

Phys.Rev.C 92 (2015) 3, 034913

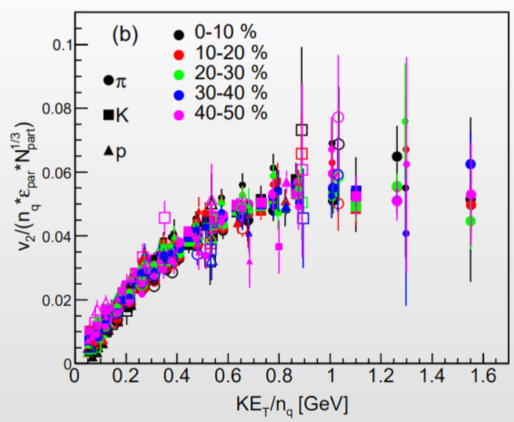

Phys. Rev. Lett. 122 (2019) 172301

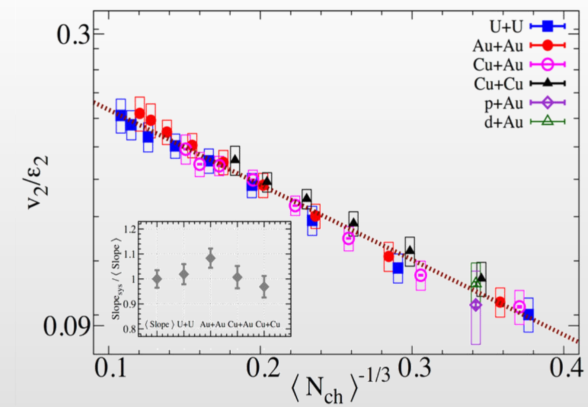

System size scan (p-A, A-A) is an important ingredient:

initial geometry → flow harmonics → $\boldsymbol{\frac{\eta}{s}(T,\mu), \frac{\zeta}{s}(T,\mu), c_s(T), \alpha_s(T), etc.}$

MPD performance for v_1, v_2 of V0 particles

❖ BiBi@9.2 GeV (PHSD, 15M), full event reconstruction

Differential flow can be defined using the following fit:

$$v_n^{SB}(m_{inv}) = v_n^S \frac{N^S(m_{inv})}{N^{SB}(m_{inv})} + v_n^B(m_{inv}) \frac{N^B(m_{inv})}{N^{SB}(m_{inv})}$$

- v_n^S - signal anisotropic flow (set as a parameter in the fit)
- $v_n^B(m_{inv})$ - background flow (set as polynomial function)

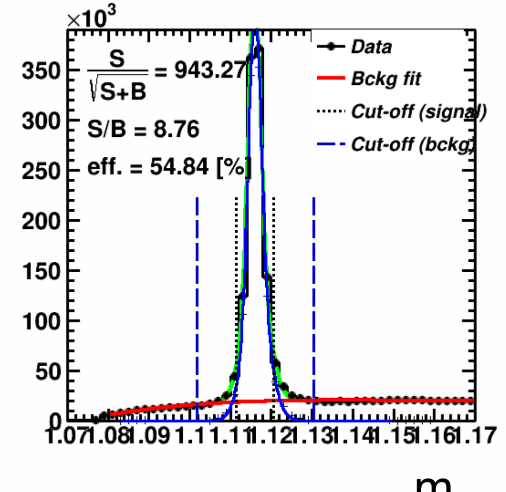

❖ Performance of v_1 and v_2 of Λ hyperons:

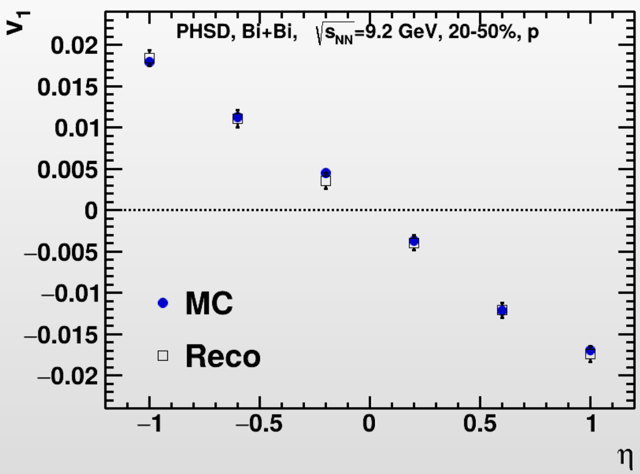

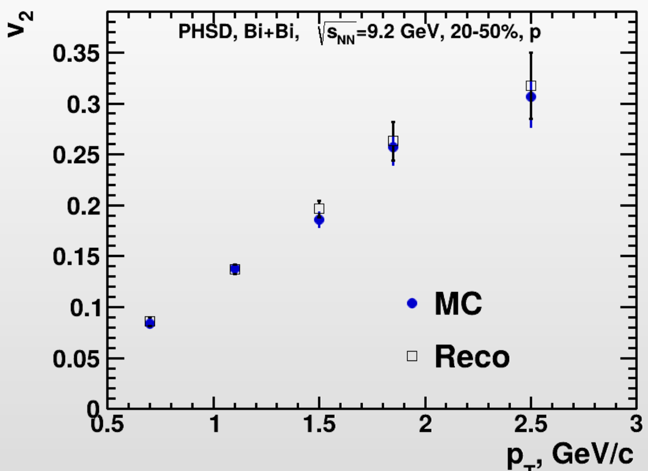

❖ Good performance for v_1, v_2 using invariant mass fit and event plane methods

❖ Similar measurements for Ks, other hyperons and short-lived resonances

MPD performance for v_1, v_2 of π/K/p

❖ BiBi@9.2 GeV (UrQMD, 50M), full event reconstruction

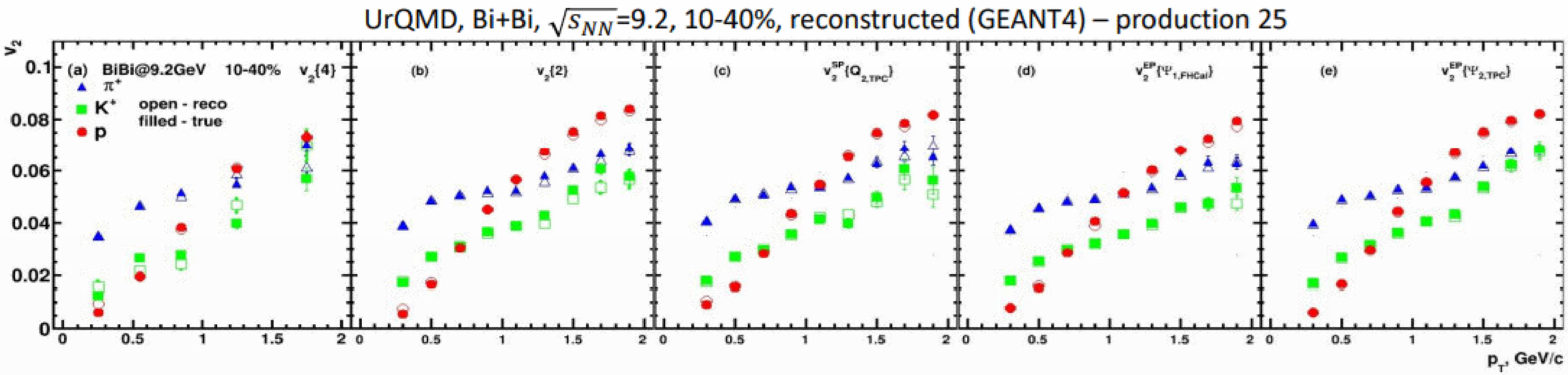

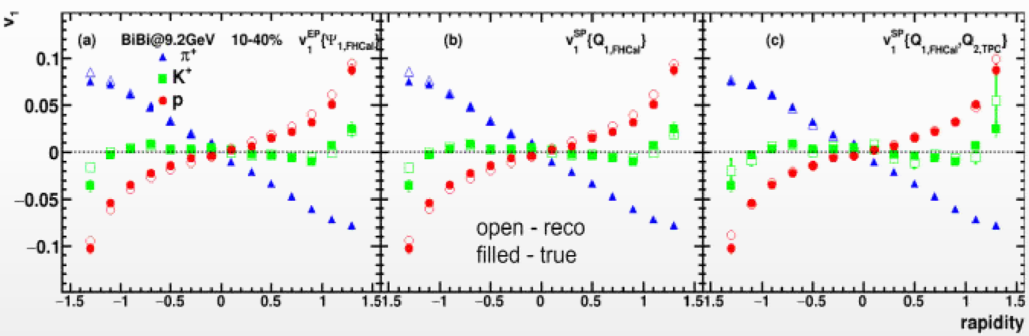

❖ Reconstructed and generated v_1 and v_2 for identified hadrons are in good agreement for all methods

MPD has capabilities to measure different flow harmonics for a wide variety of identified hadrons

System size scan for flow measurements is vital for understanding of the medium transport properties and onset of the phase transition

Hydrodynamic model

- Calculations were done using **UrQMD hydro model**
- We consider two scenarios of hydrodynamic evolution:
  - Thermalized hot dense nuclear matter with a first-order phase transition from QGP to hadronic phase **Bag model EoS**
  - Hadron gas including the same degrees of freedom as UrQMD (hadrons with masses up to 2.2 GeV) **HG EoS**
- We used **out-side-long parametrization** of relative momentum (and corresponding observables):
  - out – direction along the transverse momentum
  - long – along the longitudinal momentum
  - side – perpendicular to previous directions

$$K^\mu = (K^0, K_\perp, 0, K^z), \quad q^\mu = (q^0, q_o, q_s, q_l), \quad \Rightarrow \quad q_\mu K^\mu = 0 \quad \Rightarrow \quad q_o = (\boldsymbol{q}_\perp \cdot \boldsymbol{K}_\perp)/K_\perp, \; q^0 = \frac{\boldsymbol{q} \cdot \boldsymbol{K}}{K^0}, \quad q_s = |\boldsymbol{q}_\perp - (\boldsymbol{q}_\perp \cdot \boldsymbol{K}_\perp)\boldsymbol{K}_\perp / K_\perp^2|, \quad q_l = q_z. \quad \Rightarrow \quad R_s^2 = \langle x_s^2 \rangle, \quad R_o^2 = \langle (x_o - \beta_T t)^2 \rangle, \quad R_L^2 = \langle (x_l - \beta_L t)^2 \rangle$$

both photons are on mass shell

- For each cell in hydro calculations emission rates of thermal photons are calculate according to functions from previous slide:
  - estimation of thermal photon yields for given p_T (K_T) and φ in lab system **integration** over all cells and evolution time

Dielectron continuum and LVMs

- The QCD matter produced in A-A interactions is transparent for leptons, once produced they leave the interaction region largely unaffected + not sensitive to collective expansion
- Dielectron continuum carries a wealth of information about reaction dynamics and medium properties

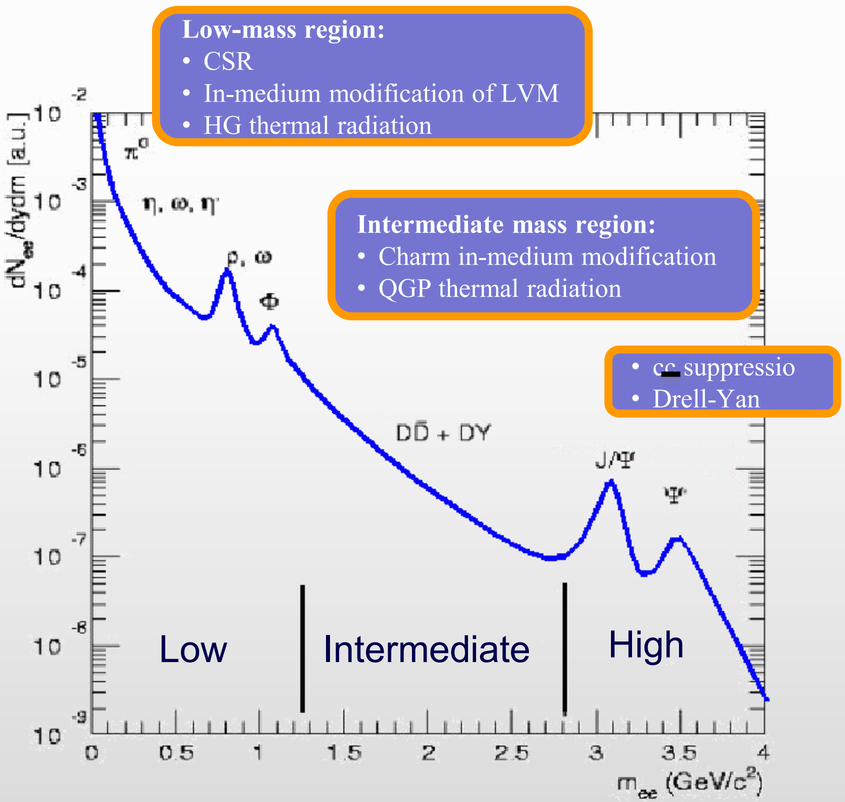

LMR as chronometer

PLB 753, 586 (2016)

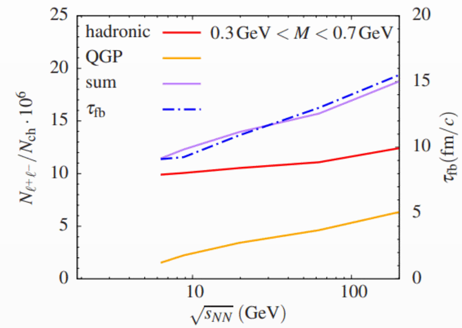

Integrated thermal excess radiation
tracks the total fireball lifetime within ~ 10% →
non-monotonous lifetime variations trace critical phenomena

IMR as thermometer

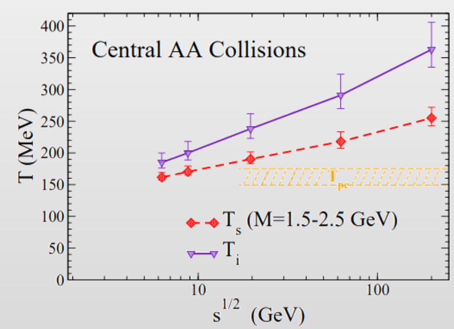

$dR_{ll}/dM \propto (MT)^{3/2}\exp(-M/T_s)$,
T_s smoothly evolves T = 160 MeV to 260 MeV

e-ID with MPD

❖ eID with TPC + TOF

n-sigma dE/dx parameterization

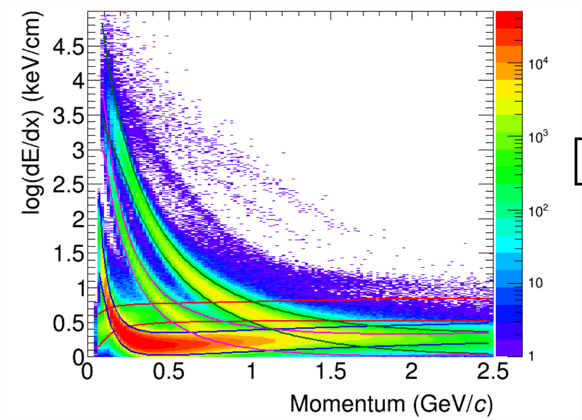

n-sigma β-TOF parameterization

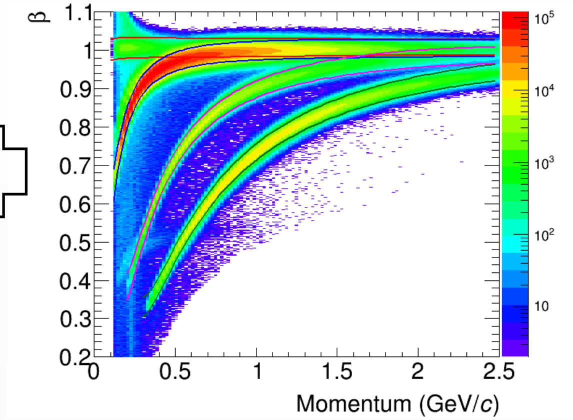

n-σ dE/dx distribution for tracks matched to TOF and identified as electrons

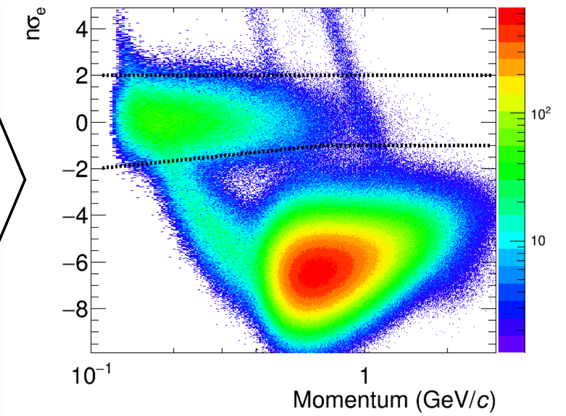

❖ eID with ECAL: steps in at higher energies where TPC/TOF become less effective

E/p for electron tracks

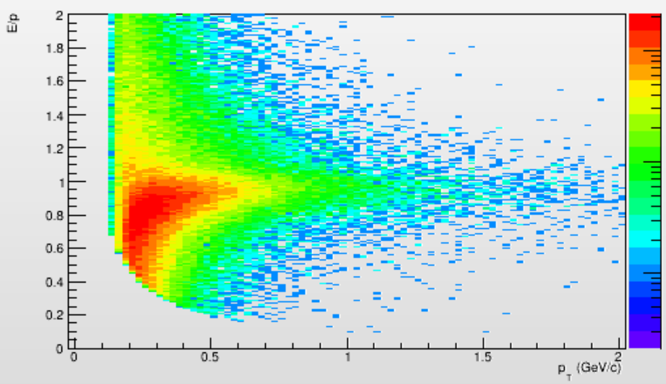

- ECAL e-ID for 2σ-matched tracks:
  - ✓ **TOF** < 2 ns (δ ~ 500 ps)
  - ✓ E/p ~ 1
- Turns on at p_T > 200 MeV/c

(Di)electrons

- Dielectron spectra are sensitive probes of the deconfinement and the chiral symmetry restoration
- AuAu@11 GeV (UrQMD for background & PHQMD for signal)

$n\cdot\sigma_e^{TPC}$ with $2\sigma_e$ PID in the TOF

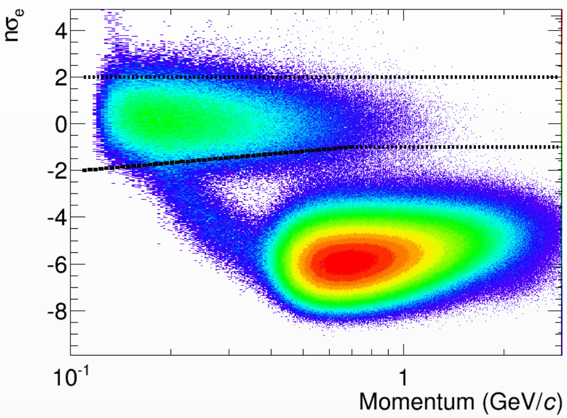

Efficiency of e-track reconstruction

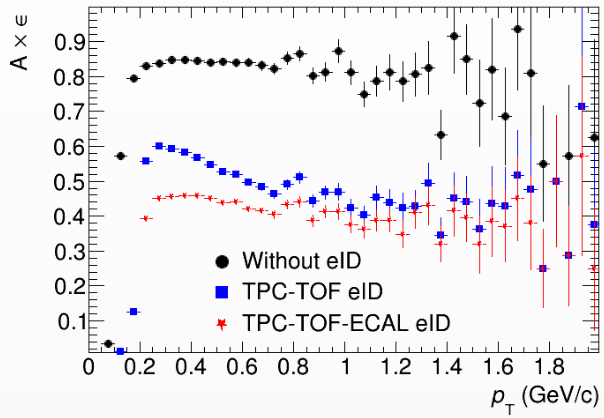

Electron purity

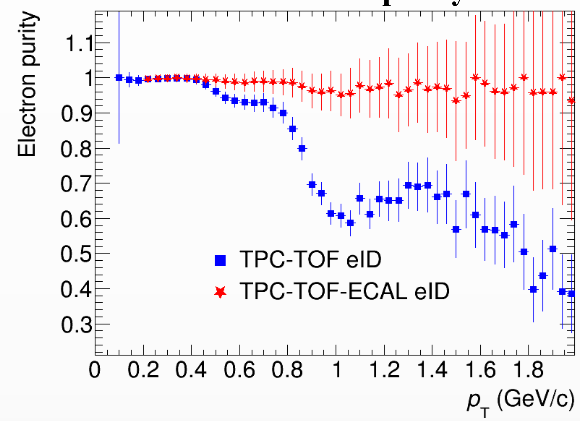

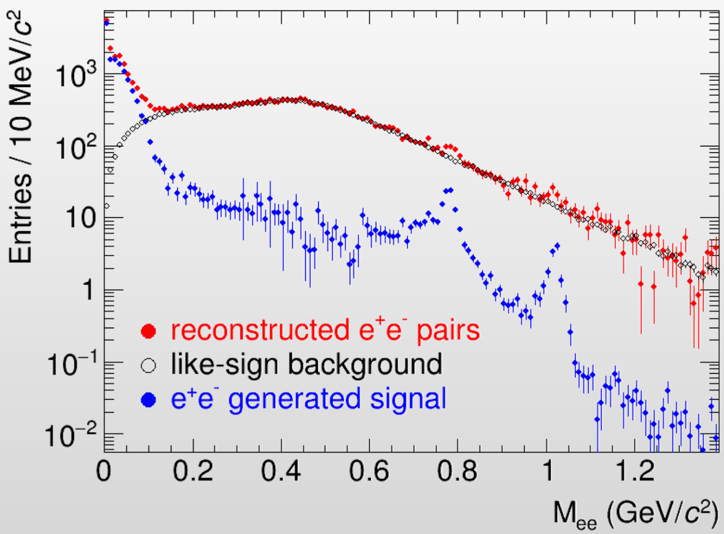

- S/B (integrated in 0.2-1.5 GeV/c^2) ~ 5-10%
- Methods to improve S/B ratio while preserving reasonable efficiency for the pairs are being developed and matured